

A GIS and statistical approach to identify variables that control water quality in hydrothermally altered and mineralized watersheds, Silverton, Colorado, USA

Douglas B. Yager · Raymond H. Johnson ·
Barnaby W. Rockwell · Jonathan Saul Caine ·
Kathleen S. Smith

Received: 22 May 2012 / Accepted: 11 December 2012 / Published online: 12 February 2013
© The Author(s) 2013. This article is published with open access at Springerlink.com

Abstract Hydrothermally altered bedrock in the Silverton mining area, southwest Colorado, USA, contains sulfide minerals that weather to produce acidic and metal-rich leachate that is toxic to aquatic life. This study utilized a geographic information system (GIS) and statistical approach to identify watershed-scale geologic variables in the Silverton area that influence water quality. GIS analysis of mineral maps produced using remote sensing datasets including Landsat Thematic Mapper, advanced spaceborne thermal emission and reflection radiometer, and a hybrid airborne visible infrared imaging spectrometer and field-based product enabled areas of alteration to be quantified. Correlations between water quality signatures determined at watershed outlets, and alteration types intersecting both total watershed areas and GIS-buffered areas along streams were tested using linear regression analysis. Despite remote sensing datasets having varying watershed area coverage due to vegetation cover and differing mineral mapping capabilities, each dataset was useful for delineating acid-generating bedrock. Areas of quartz–sericite–pyrite mapped by AVIRIS have the highest correlations with acidic surface water and elevated iron and aluminum concentrations. Alkalinity was only correlated with area of acid neutralizing, propylitically altered bedrock containing calcite and chlorite mapped by AVIRIS. Total watershed area of acid-generating bedrock is more significantly correlated

with acidic and metal-rich surface water when compared with acid-generating bedrock intersected by GIS-buffered areas along streams. This methodology could be useful in assessing the possible effects that alteration type area has in either generating or neutralizing acidity in unmined watersheds and in areas where new mining is planned.

Keywords Watershed · Hydrothermal alteration · Water quality · GIS · Statistical analysis

Introduction

Abandoned mine lands (AML) investigations conducted by the U.S. Geological Survey between 1996 and 2001 in the Animas River watershed (ARW) near Silverton, Colorado, USA, resulted in one of the most comprehensive geodatasets for a watershed affected by hard-rock metallic mining (Church et al. 2007). Information on ARW geology, geophysics, geochemistry, hydrology, biology, remote sensing, base geographic, and digital terrain information is archived in a relational database and in geographic information system (GIS) coverage formats (Yager and Bove 2007; Sole and Rich 2007; Smith et al. 2007; Kimball et al. 2007; Bove et al. 2007a, b; Dalton et al. 2007). Several AML datasets were analyzed for this study. Federal land managers and the local ARW Stakeholders group are actively involved in remediation of abandoned mines in the ARW, a region that was the site of base-metal (Cu–Pb–Zn) and precious-metal (Ag–Au) hard rock mining from the late 1870s to 1991. An extensive legacy of mining has left behind hundreds of mines and prospects. Weathering of mine waste and hydrothermally altered bedrock that hosts the metallic mineral deposits causes oxidation of sulfide minerals forming acidic and metal-rich leachate that

Electronic supplementary material The online version of this article (doi:10.1007/s12665-013-2229-y) contains supplementary material, which is available to authorized users.

D. B. Yager (✉) · R. H. Johnson · B. W. Rockwell ·
J. S. Caine · K. S. Smith
U.S. Geological Survey, Denver, CO, USA
e-mail: dyager@usgs.gov

adversely impacts water quality and is toxic to aquatic life (Church et al. 2007; DeGraff 2007).

A principal goal of this study was to analyze AML datasets to advance our understanding of the physical factors that control water quality at the watershed scale (1.5–20 km²). Knowledge of the most important variables that produce acid rock drainage (ARD) is especially useful to land managers and mining companies to aid in identifying areas posing the greatest environmental risks where new mining will occur and that may present reclamation challenges once mining ceases. In contrast, when watersheds have physical variables that can reduce acidity, such as rocks with acid neutralizing capacity (ANC), this information is also useful in mine site planning and remediation efforts, as it can be used to help mitigate acid mine drainage and sequester metals (Yager and Caine 2003; Yager et al. 2005, 2008a, b).

Geographic and geologic setting

The San Juan Mountains exhibit a wide diversity of ecological characteristics due to their mid-latitude location, high elevation, extreme topographic relief, and consequent ecosystem variability. The San Juan Mountains encompass subalpine parks, grasslands, and wetlands that contain multiple ecosystems including alpine, spruce fir; mixed conifer, ponderosa pine, oak, Douglas fir, and aspen forests; parks and meadowlands, mountain shrub, and pinon-juniper woodlands; and shrub-steppe communities (Chapman et al. 2006). Relatively high regional precipitation, occurring primarily as snow in the fall and winter, results in the critical water recharge area to the semi-arid Colorado River basin.

The geology of the western San Juan Mountains study area is exceptional in that many diverse rock types representing geologic eras from the Precambrian to Cenozoic are preserved. The general stratigraphy of the study area consists of Precambrian crystalline basement rocks overlain by Paleozoic to Tertiary sedimentary rocks and a voluminous Oligocene volcanic cover (Yager and Bove 2007). The volcano-tectonic framework of the study area consists of early intermediate composition volcanism overprinted by caldera-forming eruptions. An arcuate primary drainage network delineates structural margins of the San Juan and the nested Silverton calderas (Fig. 1). Structures that developed coincident with caldera collapse served as flow paths for hydrothermal fluids during several episodes of hydrothermal alteration and base- and precious-metal mineralization (Casadevall and Ohmoto 1977; Bove et al. 2001; Yager and Bove 2007). The northeast-trending Eureka graben served as an important flow path for mineralization and formed in response to caldera resurgence of the San Juan and Silverton caldera complex. Where not locally overprinted by intense hydrothermal

alteration, a regional propylitic alteration assemblage containing calcite, chlorite, and epidote pervades the entire study area, locally supplying ANC and alkalinity to surface water (Yager et al. 2005, 2009; Yager 2008). The study area was extensively glaciated during the Pleistocene epoch and has high topographic relief ranging in elevation from 2,800 m to over 4,200 m providing for excellent bedrock exposures.

Previous work

Geochemical investigations in the study area

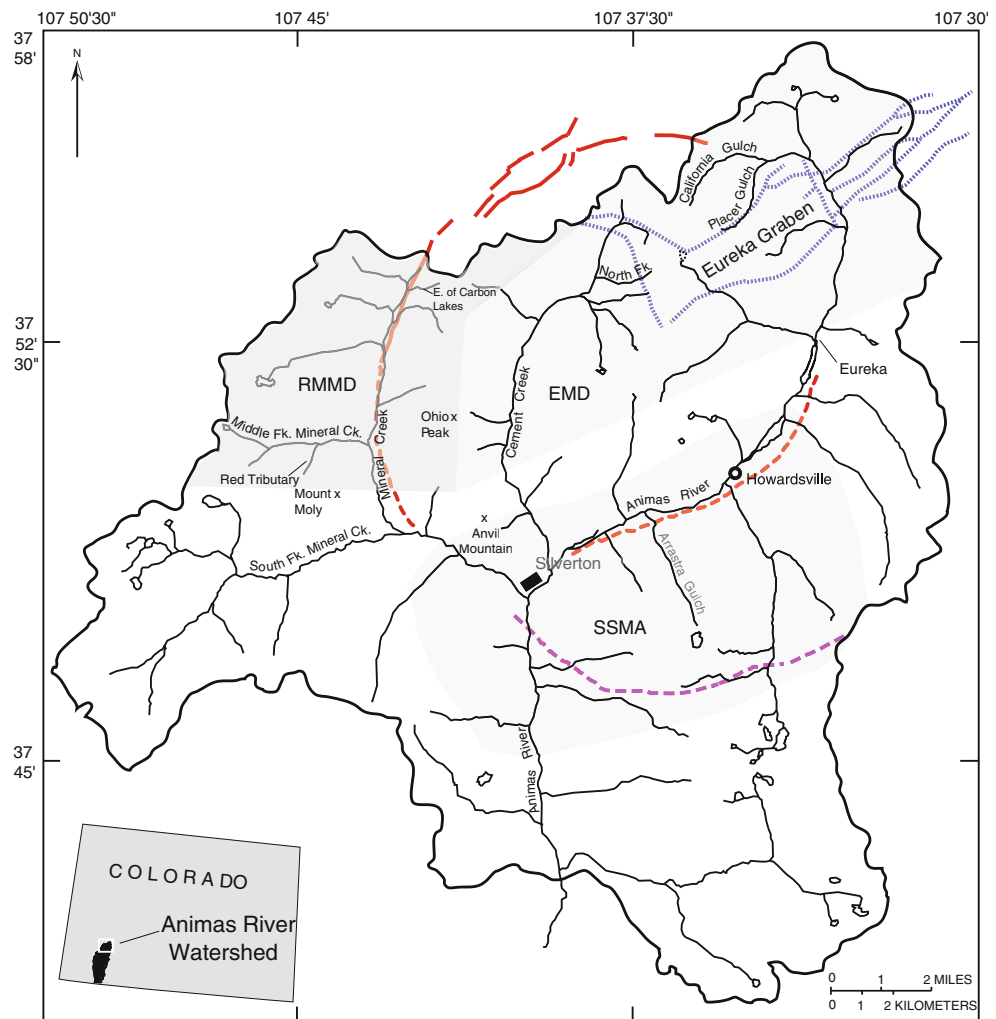
Issues addressed as part of past AML research included identifying the relative contributions of ARD and associated metal loads to surface water from mined watersheds and naturally altered and unmined areas. Research described in Bove et al. (2007b) focused on determining water quality geochemical characteristics of surface water and groundwater that is sourced in rocks having well-characterized geologic units and hydrothermal alteration types. Water sampled as part of the Bove et al. (2007b) study was classified as being either mining- or non-mining affected. Statistics were used to indicate the range in concentration for multiple metals, sulfate, and pH. The study characterized the chemistry of waters sourced in highly and weakly altered rock types, but no attempt was made to determine how watershed water chemistry might be influenced as a function of differing proportions and types of watershed variables. Mast et al. (2000b) used a geochemical mass-balance approach to determine that un-mined, hydrothermally altered watersheds can contribute as much as 56–90 % of dissolved metal loads to surface waters, but the possible influences of multiple geologic watershed variables on water quality were not assessed.

GIS and statistical approaches used for other study areas

Previous studies in other areas have utilized watershed-based GIS and statistical approaches to evaluate the influences of watershed physical characteristics on water quality. Wang and Yin (1997) used GIS to assess the effects of variable land use and land cover type on surface water quality. Investigations in subalpine to alpine areas have addressed the influence that terrain slope, vegetation, surficial deposits, and bedrock lithology have on water quality (Clow and Sucker 2000). Sliva and Williams (2001) used analysis of entire watershed area and a linear GIS stream buffer to assess influences of land use types on water quality.

A watershed-based and statistical approach was used in the central Colorado Rocky Mountains by Schmidt et al.

Fig. 1 Location map of the Animas River watershed study area showing geographic features discussed in text. *Shaded areas* are *RMMD* Red Mountain mining district, *EMD* Eureka mining district, and *SSMA* South Silverton mining area. Note that E. of Carbon Lakes and Red Tributaries are informal names used to describe features discussed in the text. *Red line* Silverton caldera structural margin, *purple dashed line* San Juan caldera southern topographic margin



(2009, 2010), which includes GIS analysis of generalized alteration types derived from analysis of advanced spaceborne thermal emission and reflection radiometer (ASTER) data, water quality determined for samples collected at watershed outlets, and macro benthic invertebrate data as an indicator of ecosystem health. Their work identifies inverse correlations between area of hydrothermal alteration and macro benthic taxa type and abundance. An approach similar to that of Schmidt et al. (2009) was used by Bruns (2005), who developed a GIS and statistical analysis methodology of watersheds to understand stream ecosystem response to potential land use impacts caused by coal mining in northeastern Pennsylvania and southern New York.

Methodology and datasets

Methods used in this study combined a GIS and a statistically based approach that builds on preliminary work

(Yager et al. 2002; Yager and Caine 2003; Yager et al. 2008a, b). In this study, GIS was used to analyze digital terrain surfaces to create derivative watersheds and hydrologic stream networks that, in turn, could be used to analyze AML geology and alteration datasets in a geochemical and geologic context. The watersheds are used as a geographic frame of reference for determining area of geologic units and alteration types.

Work completed as part of this study differs from previous research in that data acquired using GIS analysis of geologic and detailed alteration maps completed during AML investigations (Bove et al. 2007a; Yager and Bove 2007) were used to test statistical correlations between water quality signatures and hydrothermal alteration mapped using three different remote sensing platforms. The remote sensing datasets utilized in this study included: (1) Landsat Thematic Mapper (TM) (Rockwell 2010), (2) ASTER (Rockwell 2010), and (3) Airborne Visible Infrared Imaging Spectrometer (AVIRIS) (Bove et al. 2007a).

Geomorphometric and GIS methods

A surface hydrologic modeling tool, the GIS Weasel (Viger et al. 1998; Viger and Leavesley 2007; Viger 2008), was used to analyze a 10 m resolution USGS digital elevation model (DEM) and extract watershed data including slope, aspect, flow direction, flow accumulation, and drainage network grids. Standard DEM preprocessing commands available in ArcGrid™ were utilized that are accessed by the GIS Weasel software application. The DEM preprocessing steps (*fill*, *flow direction*, and *flow accumulation*) are required for subsequent geomorphometric analysis because these functions control how hydrologic flow is routed on a digital surface having grid-cell *x*–*y* coordinate locations and elevation information. *Fill* is calculated using a technique described by Jensen and Domingue (1988) that locates each cell whose elevation is lower than that of eight adjacent neighboring cells and raises the elevation of these cells to that of its nearest neighbors. Once erroneous topographic depressions are corrected using *Fill*, this permits the downhill flow across a DEM to be determined. *Flow direction* is calculated from the filled DEM, using the D8 algorithm (Jensen and Domingue 1988). The *flowdirection* surface is then used to calculate a flow accumulation surface, which delineates those higher elevation cells that contribute flow to a specific grid cell (Jensen and Domingue 1988; O’Callaghan and Mark 1984). A hydrologic stream network grid was established using the *flow accumulation* (flowacc) grid and the following ArcGrid™ conditional (con) function:

$$\text{streamnet} = \text{con}(\text{flowacc} > 1,000, 1)$$

A flow accumulation threshold of 1,000 was used in the *Streamnet* function. All 10-m resolution cells in the flow accumulation grid with more than 1,000 cells flowing into them are assigned 1, and all other cells are assigned no data. The grid-cell contributing area of 1,000 used in this study resulted in a realistic, basin-wide hydrologic network that most closely resembled the drainage network observed in the field.

The GIS Weasel software utilizes the *Watershed* function of ArcGrid™ to delineate watersheds that represent upstream contributing areas derived from a source grid (Viger and Leavesley 2007). Each delineated watershed has a unique numeric identifier that can be associated with attributes of other geodatasets and provides a basis for spatial and statistical comparisons (Fig. 2). Once watersheds were delineated, GIS Weasel parameterization routines were used to calculate areas of alteration and bedrock lithologies in each watershed derived from digital geologic and alteration maps (Yager and Bove 2007; Bove et al. 2007a). In addition, an AVIRIS-derived vegetation map (Dalton et al. 2007) was

analyzed using GIS to determine intersections between vegetated and barren areas corresponding with alteration types for each watershed. The zonal statistics function available in ArcGIS™ was used to calculate the area of each watershed alteration type derived from the ASTER and TM alteration grids. Tables of watershed alteration types were imported into Mintitab™ software for statistical analysis.

A 30-m GIS buffer was applied to the hydrologic network grid to determine areas adjacent to streams that intersect alteration types. GIS buffer-derived data were subsequently compiled for statistical comparison with results from whole watershed statistical analysis. GIS-buffered areas adjacent to a stream network could represent locations within a watershed that are more susceptible to hydrologic weathering due to sediment being transported along perennial and ephemeral stream channels where the erosive power of surface water runoff may be highest. The GIS stream buffer was only applied to the AVIRIS-based alteration map in which alteration types were extrapolated to include vegetated areas, resulting in nearly complete watershed mineral mapping coverage. The only unmapped parts of the AVIRIS-based alteration map are those areas covered by surficial deposits.

Remote sensing data

Landsat Thematic Mapper

TM measures six spectral bands between 0.4 and 2.4 μm. Bands 1, 2, and 3 overlap the visible, blue, green, and red parts of the electromagnetic spectrum between 0.4 and 0.7 μm. Bands 4 (0.7–0.9 μm), 5 (1.5–1.8 μm), and 7 (2.0–2.4 μm) measure in the near- to shortwave infrared (SWIR) parts of the spectrum. Absorption spectra detected by TM are too broad to delineate specific minerals, but the spectra do permit mineral groups such as clays and iron minerals important in hydrothermally altered areas to be mapped. The spatial resolution for TM data is 30 m. In the Animas River study area, only 2–3 % areas above tree-line that are devoid of vegetation are adequately exposed for TM mineral group mapping. TM band ratios are used to reduce the effect of uneven illumination and enhance spectral contrast (Rockwell 2010). A compound ratio of (5/7–4/3) was used to delineate the clay–sulfate–sericite minerals. The spectral influence of chlorophyll-bearing green vegetation (highlighted by the 4/3 ratio) was removed from the 5/7 ratio results. A compound band ratio of (3/1 × (3 + 5/4)) was used to highlight ferric iron minerals having strong charge transfer absorptions in band 1 and crystal field absorptions in band 4 (Fig. 3). TM data are available for the entire United States and are, therefore, pertinent to national-scale geoenvironmental assessments.

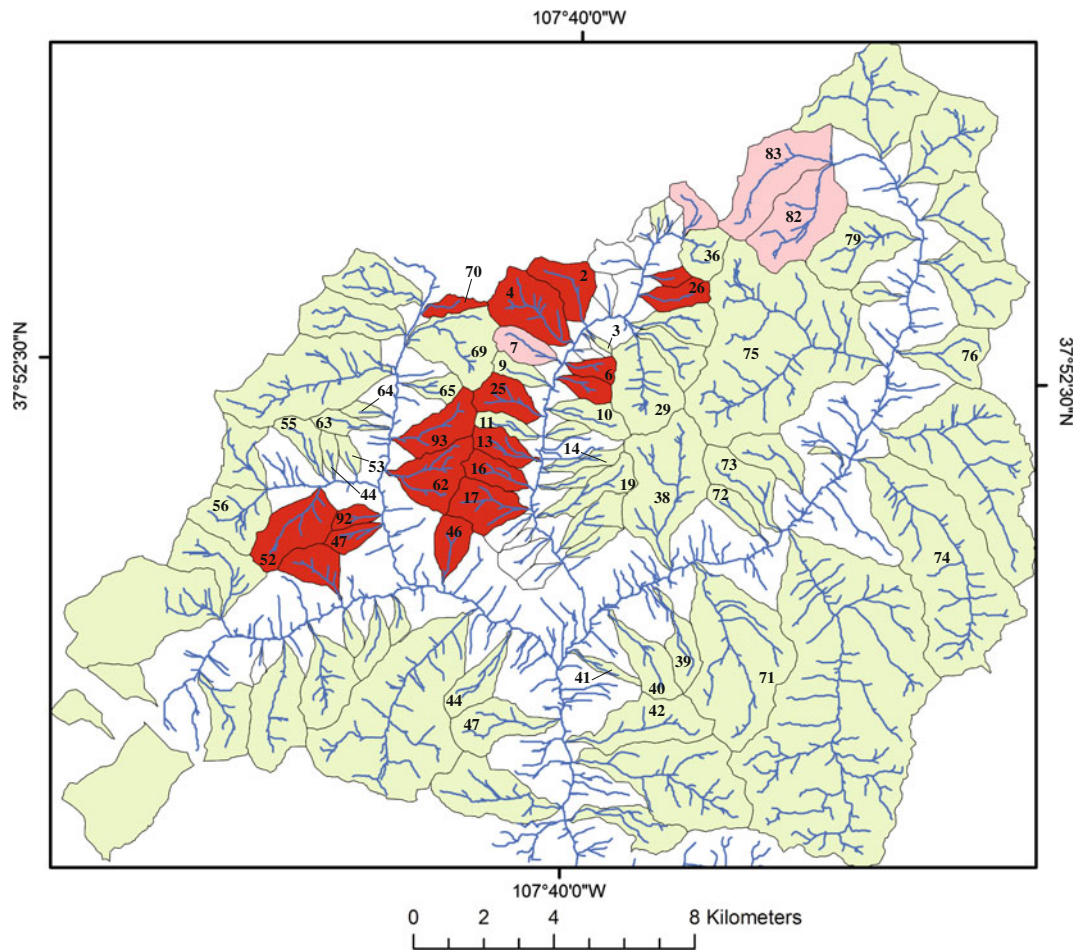


Fig. 2 Watersheds and associated id’s delineated using the GIS Weasel software interface and the ArcGrid™ watershed function. Watersheds in *green* (near neutral pH), *coral* (5.0–6 pH), *red* (<5 pH). GIS id’s are only shown for areas sampled at the watershed outlet or discussed in text. The id’s and corresponding names are listed as follows: 2 Dry Gulch, 3 South of Dry Gulch, 4 Prospect Gulch, 6 Tiger Gulch, 7 Georgia Gulch, 9 Fairview Gulch, 10 Cascade Gulch, 11 Porcupine Gulch, 13 Ohio Gulch, 14 Illinois Gulch, 16 Topeka Gulch, 17 Niagra Gulch, 19 Hancock Gulch, 25 Minnesota Gulch, 26 North Fork Cement Creek, 29 South Fork Cement Creek at Gladstone, 36 Ross basin, 38 Boulder Gulch, 39 Blair Gulch, 40 Swansea Gulch,

41 Idaho Gulch, 42 Kendall Gulch, 44 Northeast of Belcher mine, 46 Zuni Gulch, 47 Battle Ship Slide, 52 Red Tributary, 53 Middle Fork Mineral Creek (east watershed), 54 Middle Fork Mineral Creek (central watershed), 55 Middle Fork Mineral Creek (western watershed), 56 Paradise basin, 62 South of Brown’s Gulch, 63 South of Imogene Mine, 64 West of Imogene Mine, 65 Southeast of Chattanooga, 69 Big Horn Gulch, 70 Carbon Lake, 71 Arrastra Gulch, 73 Hematite Gulch, 75 Eureka Gulch, 76 Niagra Gulch (upper Animas River basin), 79 Picayune Gulch, 82 Placer Gulch, 83 California Gulch, 87 Cunningham Creek, 92 South of Bonner mine, 93 Brown’s Gulch

Alteration types mapped by TM data and area calculations determined by GIS are in Table 1.

ASTER

The ASTER sensor measures reflected solar radiation in three bands between 0.52 and 0.86 μm and six bands between 1.6 and 2.43 μm; and emitted radiation in five bands between 8.125 and 11.65 μm (ERSDAC 2005). Absorption features in the shortwave infrared spectral region between 1.0 and 2.5 μm are shown to be particularly

useful for mapping silicates and carbonates (Hunt and Salisbury 1970, 1971; Rockwell 2009). The spatial resolution for the SWIR part of the spectrum is 30 m. Vegetation cover commonly obscures 88 % of watershed areas in the Animas River study area permitting 12 % of the area to be mapped by ASTER (Fig. 4). Minerals and mineral mixtures were identified from the ASTER data using spectroscopic analysis techniques described by Rockwell (2009). The identified minerals were then combined into alteration and lithologic types using a Boolean modeling technique based on standard definitions of the alteration

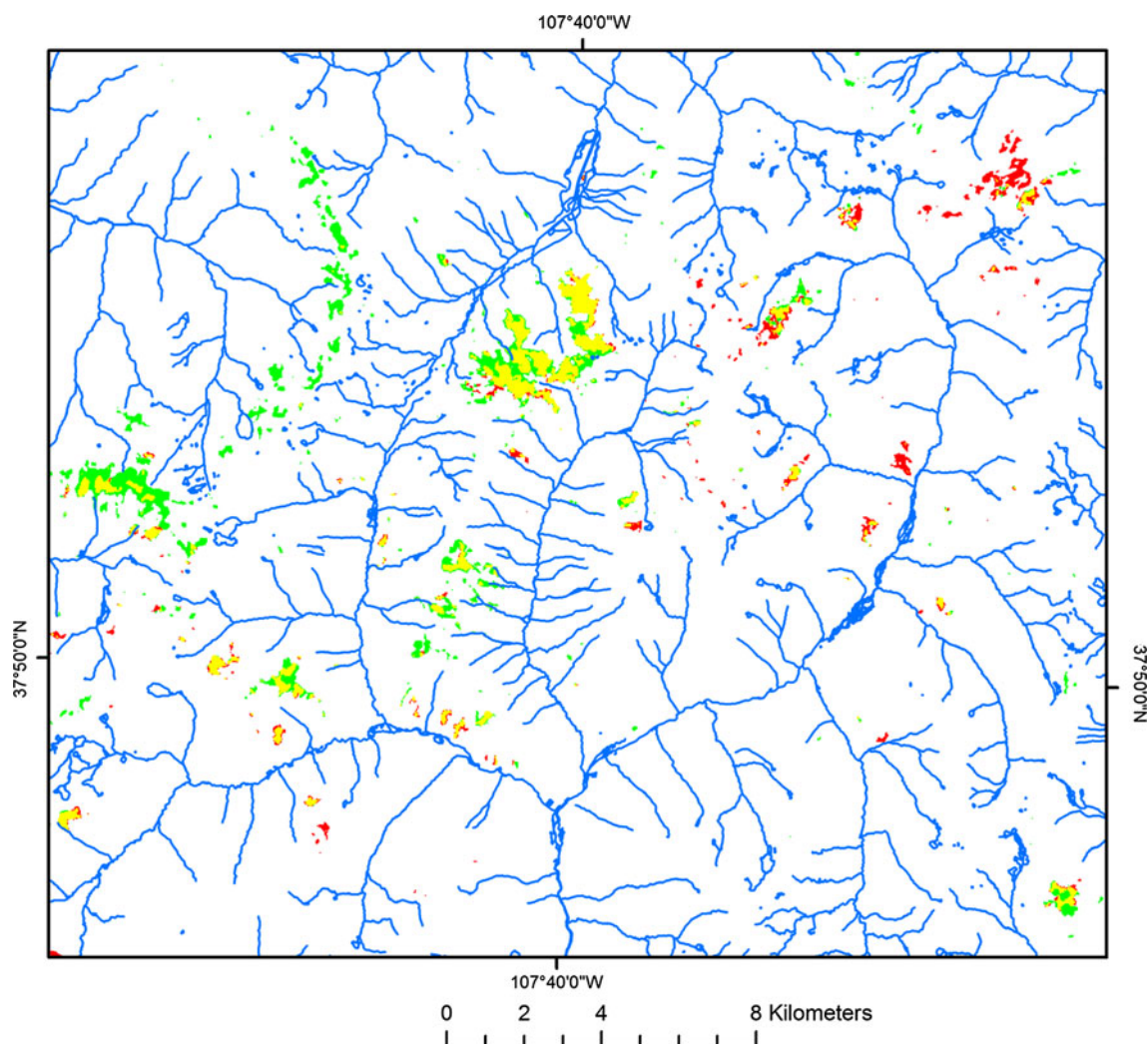


Fig. 3 Distribution of mineral groups identified using ratio-based analysis of TM data. *Yellow* ferric iron + clay-sulfate-mica, *Green* clay-sulfate-mica only, *Red* ferric iron only

mineralogy (Rockwell 2010). Modeled alteration types include separate argillic, four pyrite-bearing, and six propylitic and carbonate-bearing alteration assemblages. ASTER is available for the entire US and could be a valuable tool for mapping hydrothermal alteration as part of geoenvironmental assessments requiring coverage of large areas. Alteration types mapped by ASTER and area calculations determined by GIS are in Table 1.

Hybrid AVIRIS and field-based alteration map

In contrast to TM and ASTER, AVIRIS data are available only in selected areas of the US for detailed study of relatively small watershed areas or specific basins. A hybrid alteration map that integrates AVIRIS spectral interpretations of Dalton et al. (2007) and field-based mapping (Bove

et al. 2007a) provides nearly 100 % bedrock coverage irrespective of vegetation cover (Fig. 5). AVIRIS has 224 narrow spectral bands between 0.4 and 2.5 μm that are in the visible, near infrared and mid-infrared parts of the spectrum. The narrow spectral bands enable individual minerals to be delineated due to characteristic absorption spectra of mineral species. The AVIRIS spectra used for the hybrid alteration mapping have a spatial resolution of 17 m^2 and represent the highest resolution remote sensing dataset used in our analysis. AVIRIS mineral mapping was supplemented by field-based mapping and mineralogy studies augmented by X-ray diffraction analyses, which permitted the entire area of each watershed not covered by surficial deposits to be assigned to one of 21 alteration types (Bove et al. 2007a). This hybrid product contrasts with TM- and ASTER-derived alteration maps in which

Table 1 Alteration type area (m²) determined by GIS analysis of Landsat–TM and ASTER alteration mapping for Cement Creek, Mineral Creek, and upper Animas River basin watersheds

Basin and Watersheds	TM–clay–sulfate–sericite	TM–Fe	ASTER argillic +ferric Fe	ASTER quartz–sericite–pyrite (phyllic)	∑(all ASTER quartz–sericite–pyrite)
<i>Cement Creek basin</i>					
Dry Gulch	485,100	538,200	169,425	135,225	135,225
South of Dry Gulch	0	0	0	0	0
Prospect Gulch	361,800	633,600	166,725	165,825	165,825
Tiger Gulch	0	4,500	1,350	1,575	1,575
Georgia Gulch	26,100	70,200	1,575	0	225
Fairview Gulch	0	900	0	0	0
Cascade Gulch	0	6,300	900	675	675
Porcupine Gulch	45,000	52,200	19,575	18,900	18,900
Ohio Gulch	302,400	327,600	92,250	78,975	79,875
Illinois Gulch	0	0	2,250	1,575	1,575
Topeka Gulch	99,900	139,500	42,750	37,800	38,025
Niagara Gulch	81,900	134,100	49,500	75,825	75,825
Hancock Gulch	0	1,800	225	1,350	1,350
Minnesota Gulch	0	40,500	6,750	1,125	2,475
South Fork Cement Creek (above M. Fork)	141,300	158,400	32,850	69,750	70,650
North Fork Cement Creek	29,700	98,100	5,850	17,325	17,325
Ross basin	0	16,200	0	0	0
<i>Mineral Creek basin</i>					
Northeast of Belcher Mine	1,748,700	0	450	0	675
Zuni	1,351,800	36,900	48,375	39,600	39,825
Battleship slide	813,600	27,000	20,250	11,250	13,500
Red Tributary	2,673,900	156,600	48,600	13,050	14,625
South of Bonner Mine	612,900	900	1,125	0	0
Middle Fork Mineral Creek-East Basin	476,100	0	0	0	450
Middle Fork Mineral Creek-Central Basin	492,300	7,200	0	450	450
Middle Fork Mineral Creek-West Basin	1,165,500	34,200	6,075	2,025	2,250
Paradise Basin	2,814,300	85,500	13,275	2,025	5,175
South of Browns Gulch	2,406,600	228,600	52,425	91,800	91,800
Browns	2,124,900	75,600	18,675	24,975	24,975
South of Imogene Mine	833,400	1,800	2,475	675	675
West of Imogene Mine	409,500	0	1,575	900	900
Southeast of Chattanooga	811,800	0	1,350	1,125	1,125
Big Horn Gulch	3,865,500	15,300	10,575	0	0
East of Carbon Lake	666,000	0	2,025	1,350	1,350
<i>Upper Animas River basin</i>					
Boulder Gulch	0	0	3,150	900	1,350
Arrastra Creek	900	2,700	4,725	0	1,575
Hematite Gulch	0	900	0	0	0
California Gulch	306,900	186,300	9,225	0	1,575
Blair Gulch	0	0	0	0	225
Niagra Gulch (upper Animas)	4,500	17,100	675	0	0
Swansea Gulch	0	900	0	0	0
Eureka Gulch	98,100	254,700	9,900	0	7,200
Picayune Gulch	0	8,100	450	0	0
Placer Gulch	106,200	230,400	8,775	225	1,125

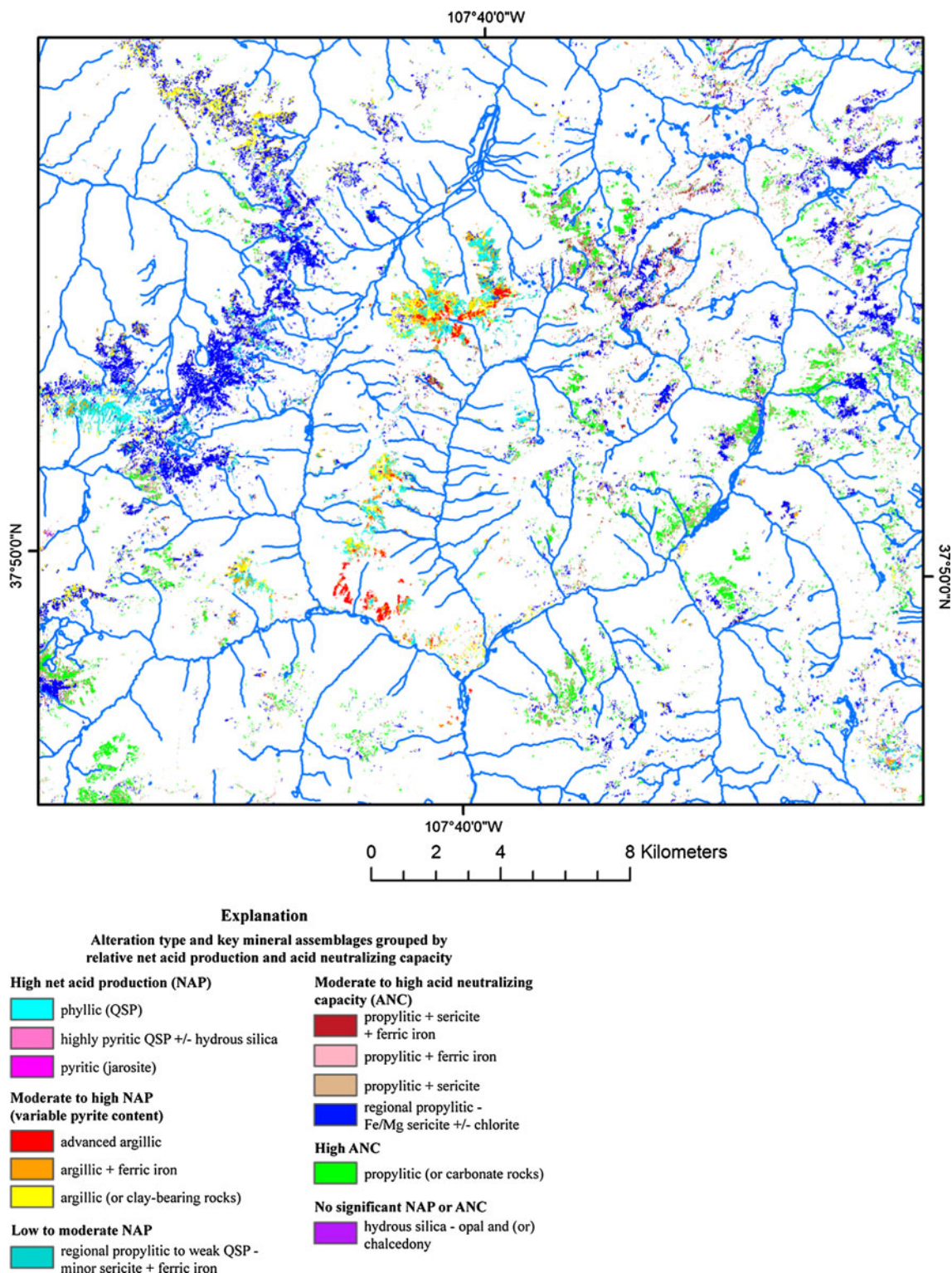


Fig. 4 Distribution of alteration mapped by ASTER that was used in GIS alteration area determinations

vegetated areas are not shown. Hydrothermally altered areas mapped with AVIRIS, however, show excellent correlation with those altered areas mapped by TM and

ASTER (Rockwell 2010). Alteration from hybrid AVIRIS-derived map and area calculations determined by GIS are in Table 2.

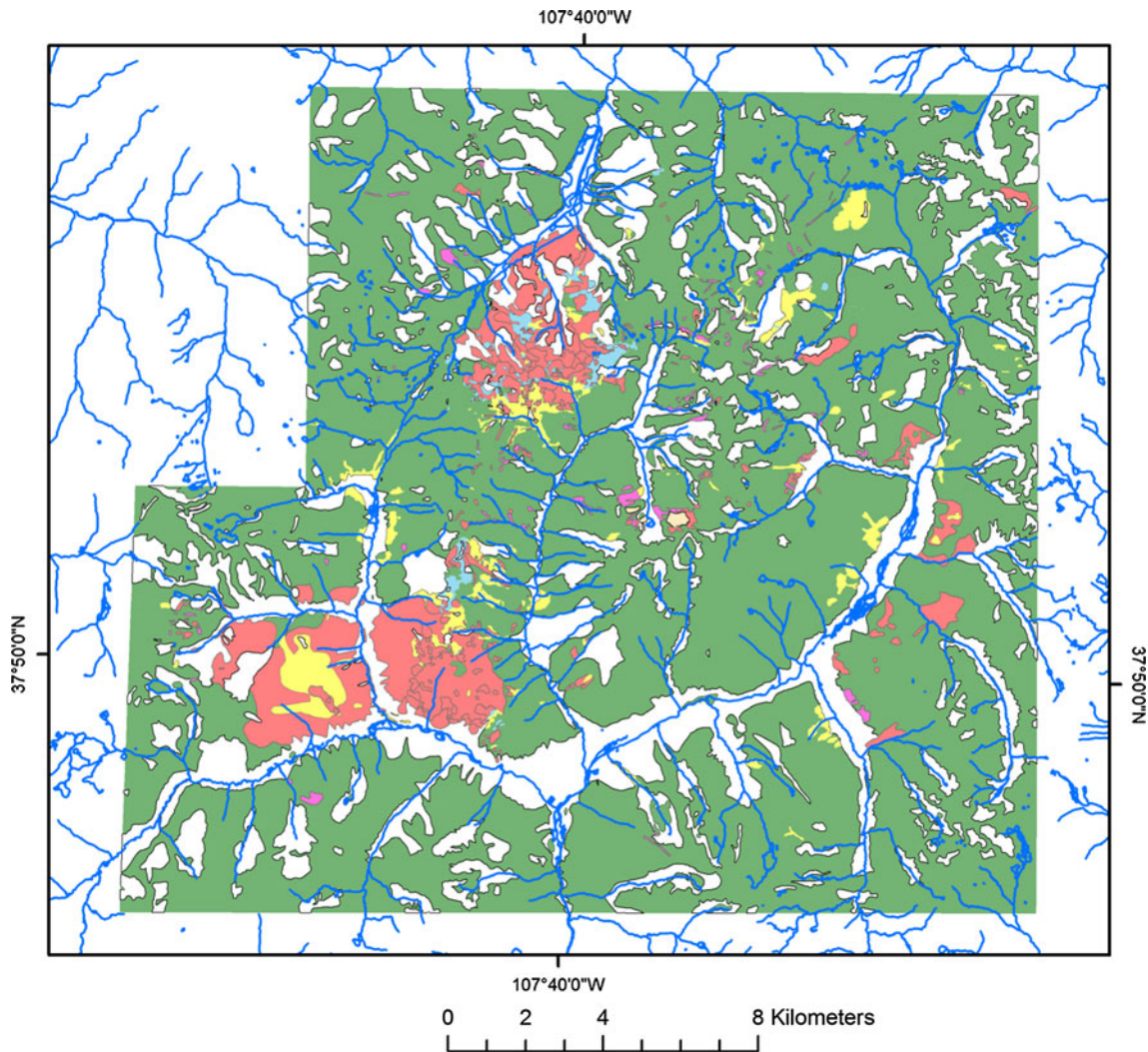


Fig. 5 Hybrid AVIRIS- and field-based map of alteration. Prevalent areas in *green* are propylitically altered rocks. *Brighter hues* represent more intense alteration that has overprinted the propylitic assemblage. A detailed geologic map (Yager et al. Yager and Bove 2007) is

available for download at <http://pubs.usgs.gov/pp/1651/downloads/>; an alteration map is described in Bove et al. (Bove et al. 2007a, 2007) and available online at <http://pubs.usgs.gov/sim/2976/>

Statistical methods

Linear regression analysis

Linear regression was used to test correlations between watershed variables (alteration type, terrain, and vegetation) and water quality signatures. The Kendall’s tau coefficient was used to measure the statistical dependence between two measured quantities—for example, the area of a specific alteration type and pH or metal concentration. Kendall’s tau is a non-parametric and statistically robust method, meaning that it does not make assumptions about a continuous probability distribution, e.g., that the data are normally distributed. The method also uses a correlation coefficient that measures the correspondence between two

rankings to assess the probability that a resultant correlation is not due to chance (Kendall 1975; Helsel and Hirsch 2002). The significance or robustness of linear dependence between two measured variables is determined using the Kendall–Theil Robust Line, which determines whether a linear regression slope coefficient for the explanatory variable is significantly different from zero (Theil 1950; Helsel and Hirsch 2002). This statistical approach tests whether variables are negatively or positively correlated, or whether there is no statistical relationship between variables. Correlation measures the co-variation between independent variables and dependent water quality parameters; however, the reasons for correlations are determined from knowledge regarding the geology and geologic processes affecting the area.

Table 2 Alteration type area (m²) determined by GIS analysis of hybrid AVIRIS mineral mapping for Cement Creek, Mineral Creek, and upper Animas River basin watersheds

Basin and Watersheds	Total area	Prop	Prop area (%)	Argillic	qsp	qap	∑(NAP)	NAP area (%)
<i>Cement Creek basin</i>								
Dry Gulch	1,980,400	658,600	33	114,000	241,300	296,600	930,675	47
South of Dry Gulch	131,600	128,100	97	0	0	0	191	0
Prospect Gulch	3,295,000	1,449,600	44	80,200	983,800	286,100	1,394,301	42
Tiger Gulch	700,100	623,000	89	0	0	0	171	0
Georgia Gulch	1,304,300	1,058,400	81	0	9,000	7,400	17,538	1
Fairview Gulch	819,300	798,100	97	0	0	0	2,371	0
Cascade Gulch	1,471,900	931,700	63	0	0	0	86,930	6
Porcupine Gulch	793,500	477,500	60	19,700	92,500	19,100	117,929	15
Ohio Gulch	1,244,900	483,900	39	71,900	280,200	104,300	427,589	34
Illinois Gulch	784,500	725,900	93	0	0	0	91,677	12
Topeka Gulch	1,291,300	894,300	69	112,000	221,400	52,800	274,334	21
Niagara Gulch	2,185,300	720,900	33	19,200	422,800	184,700	688,804	32
Hancock Gulch	1,797,300	902,900	50	0	0	0	929	0
Minnesota Gulch	1,678,200	1,505,600	90	0	0	0	3,963	0
South Fork Cement Creek (above M. Fork)	4,157,900	2,389,500	57	0	0	0	87,713	2
North Fork Cement Creek	1,198,700	730,800	61	0	0	0	112	0
Ross basin	1,605,500	1,149,600	72	0	0	0	72,828	5
<i>Mineral Creek basin</i>								
Northeast of Belcher Mine	1,752,000	1,154,100	66	0	0	0	1,034,500	0
Zuni Gulch	1,378,300	46,900	3	700	18,100	122,500	288,100	21
Battleship Slide	827,300	0	0	0	521,600	0	797,900	96
Red Tributary	3,045,600	398,800	13	0	371,300	0	1,773,400	58
South of Bonner Mine	616,000	0	0	0	148,600	0	556,700	90
Middle Fork Mineral Creek-East Basin	478,400	410,700	86	0	0	0	59,200	12
Middle Fork Mineral Creek-Central Basin	493,800	358,200	72	0	0	0	119,000	24
Middle Fork Mineral Creek-West Basin	1,170,300	761,000	65	0	0	0	2,100	0
Paradise Basin	2,995,400	1,220,000	41	0	0	0	1,651,400	55
South of Browns Gulch	2,721,800	357,800	13	164,900	156,400	69,100	619,800	23
Browns Gulch	2,267,300	1,232,500	54	63,400	38,800	1,500	115,000	5
South of Imogene Mine	834,400	484,400	58	0	0	0	0	0
West of Imogene Mine	2,267,300	1,232,500	93	63,400	38,800	1,500	115,000	5
Southeast of Chattanooga	834,400	484,400	95	0	0	0	0	0
Big Horn Gulch	402,900	376,500	98	0	13,800	0	13,800	3
East of Carbon Lake	816,600	773,500	95	0	19,700	0	19,700	2
<i>Mineral Creek basin</i>								
Boulder Gulch	6,770,200	5,592,700	83	0	0	0	0	0
Arrastra Creek	10,387,000	7,888,200	76	0	0	0	107,500	1
Hematite Gulch	2,380,700	2,352,600	99	0	0	0	0	0
California Gulch	4,968,700	3,251,800	65	6,300	297,600	0	486,200	10
Blair Gulch	1,563,000	914,500	58	0	0	0	0	0
Niagra Gulch (upper Animas)	2,518,900	1,624,800	64	0	0	0	45,000	2
Swansea Gulch	2,130,500	1,053,100	49	0	0	0	65,900	3
Eureka Gulch	19,357,000	15,235,600	79	0	0	0	278,500	1
Picayune Gulch	4,181,000	3,413,400	82	0	0	0	1,000	0
Placer Gulch	480,470	3,326,900	69	28,800	142,200	0	622,100	13

Factor analysis

Factor analysis was completed on the remote sensing alteration datasets derived from TM, ASTER, and AVIRIS data, and associated watershed water quality parameters. Factor analysis was used to help identify distinct patterns of occurrence and relationships among multiple variables that could synergistically affect watershed surface water quality. The principal component analysis extraction method was applied to the datasets, which seeks a linear combination of variables such that the maximum variance is extracted from the variables. The maximum variance is removed and analysis proceeds iteratively until the desired number of factors is extracted. This method seeks the fewest factors that can explain the variance (correlation) of a set of variables. Factor loadings ($1-n$) are the correlation coefficients between variables (rows) and factors (columns). Rotated factor loading scores were used that enable groups of interrelated data to be determined. The squared factor loading is the percent of variance in that indicator variable explained by the factor and is equivalent to Pearson's r (Helsel and Hirsch 2002).

Water quality data

Watershed and GIS-buffered area characteristics compiled using GIS were statistically evaluated to determine correlations between watershed physical properties and associated water quality signatures. Water quality analyses used for statistical comparisons were determined for samples collected at watershed outlets during synoptic sampling events (Table 3). A watershed outlet is defined as the lowest elevation location that can be sampled prior to surface water entering a main stem stream. The water quality determined at a watershed outlet represents a geochemical integration of all upstream water–rock–soil–sediment–atmosphere interactions and processes (Fig. 6).

The primary source of water quality data used in this analysis is from a relational database described in Sole and Rich (2007) and was populated from data collected as part of AML investigations (Mast et al. 2000a, 2007; Leib et al. 2007; Kimball et al. 2007; Wright et al. 2007). Samples collected during base-flow conditions during late summer to fall, primarily between 1996 and 2002, were used for analysis. Water quality samples collected during base flow conditions have element concentrations that are relatively unaffected by snowmelt dilution and are thought to closely represent groundwater discharge to streams.

Results

GIS-derived statistics for primary rock units

GIS was used to analyze AML geodatasets to determine area of bedrock units, alteration types, and vegetation coverage for each watershed. The study area consists of 63 % igneous bedrock terrain. Paleozoic, Mesozoic, and Tertiary sedimentary rock units represent 6 % of the study area. Precambrian crystalline bedrock exposed primarily along the southern caldera margins represent 4 % of outcrops. Extensive, quaternary sedimentary deposits cover 26 % of the study area and range in thickness from a few meters to more than 30 m (Yager et al. 2000; Johnson and Yager 2006; Johnson 2007).

The most widespread igneous rock type is the Silverton Volcanics intermediate composition lavas and volcanoclastic units that form 52 % of the igneous rocks and that are host to 90 % of metallic mineral deposits (Bejnar 1957). Silverton Volcanics lava filled the area of subsidence caused by San Juan caldera collapse (Yager and Bove 2002, 2007). Intermediate composition volcanoclastic deposits and minor lava flows of the San Juan Formation, exposed primarily outside the Silverton and San Juan caldera margins, represent 28 % of the igneous rocks and are the second-most abundant igneous unit. Granitoid intrusive rocks of the Sultan Mountain Stock are preserved along the western and southern caldera structural margins and comprise 8 % of the igneous rock units. The rhyolite to dacite composition Eureka Member of the Sapinero Mesa Tuff, derived from the San Juan caldera, represents 6 % of the igneous rock units and is exposed along the southern caldera margins and along the Eureka graben.

GIS-derived statistics for alteration types

During AML investigations, AVIRIS- and field-based mineral mapping permitted 21 acid-generating alteration types to be identified (Bove et al. 2007a). GIS-derived area determinations from the AVIRIS data for the principal, acid-generating alteration types determined in the Bove et al. (2007a) study are listed in order of decreasing area and are as follows: (1) propylitic acid sulfate (prop-as: 22 %); (2) quartz–sericite–pyrite (qsp: 17 %); (3) weak sericite–pyrite–hydrothermal (wsp-hyd: 17 %); (4) quartz–alunite–pyrophyllite (qap: 6 %); (5) weak sericite–pyrite–propylitic (wsp-prop: 6 %); (6) Quaternary quartz–alunite–sericite (Qqas: 6 %); (7) mixed quartz–alunite and quartz–alunite–pyrophyllite (qap-s: 5 %); (8) weak sericite–pyrite (wsp: 4 %), and (9) argillic (arg: 4 %) (Table 1, ESM only). For a detailed discussion of the alteration types listed above the reader is referred to Bove et al. (2007a).

Table 3 Water quality parameters for samples collected at watershed outlets in the Upper Animas River, Cement Creek, and Mineral Creek basins during base-flow conditions

Basin and Watershed	Date	pH	SpC	Al	Fe	Cu	Zn	SO ₄	Alkalinity
<u>Cement Creek basin</u>									
Dry Gulch	09/26/97	3.89	89	907	155	36	91	22	N.A.
South of Dry Gulch	09/20/1996	5.74	841	2,030	4,450	35	888	400	N.A.
Prospect Gulch	09/08/1997	3.22	526	11,500	26,800	136	1,130	227	N.A.
Tiger Gulch	09/20/1996	3.23	1,410	5,540	15,500	1	583	667	0.1
Georgia Gulch	09/25/1997	5.86	205	43	55	10	424	95	1.4
Fairview Gulch	09/26/1997	7.5	113	40	30	4	20	30	27.5
Cascade Gulch	09/04/1997	7.96	243	40	30	4	20	82	29
Porcupine Gulch	09/29/1997	6.38	655	86	3,200	4	930	325	11.1
Ohio Gulch	09/20/1996	3.04	980	11,200	25,300	161	1,040	356	0.1
Illinois Gulch	09/04/1997	7.91	162	40	30	4	20	45	29
Topeka Gulch	09/20/1996	4.88	1,090	4,160	4,270	28	198	597	10
Niagara Gulch	9/28/1997	3.51	247	2,930	2,040	20	93	65	N.A.
Hancock Gulch	9/20/1996	7.32	195	42	27	3	38	29	92
Minnesota Gulch	9/20/1996	4.19	353	1,830	1,210	66	408	176	0.1
South Fork Cement Creek (at Gladstone)	08/17/1999	6.34	344	196	998	10	366	147	1
North Fork Cement Creek	09/07/91	3.1	353	8,400	16,000	1,400	4,200	N.A.	N.A.
Ross basin	09/10/1997	6.17	199	109	10	66	1,200	90	2.1
<u>Mineral Creek basin</u>									
Northeast of Belcher Mine	09/13/1999	7.10	185	15	5	1	211	59	22
Zuni Gulch	08/25/1999	3.90	48	315	99	19	20	10	N.A.
Battle Ship Slide	09/15/1999	3.79	220	3,850	2,840	75	127	70	0.01
Red Tributary	10/02/1998	3.32	1,410	54,000	69,300	21	354	780	
South of Bonner Mine	09/03/1998	3.45	471	2,820	2,210	13	90	171	N.A.
Middle Fork Mineral Creek-East Basin	09/19/1995	6.78	180	1	1	2	5	68	17
Middle Fork Mineral Creek-Central Basin	09/14/1995	6.56	106	1	1	1	1	25	23
Middle Fork Mineral Creek-West Basin	09/20/1995	8.02	143	30	1	1	1	28	39
Paradise Basin	08/27/1998	6.86	566	100	310	4	52	263	9.5
South of Browns Gulch	08/25/1999	3.25	311	5,510	2,160	78	38	98	
Browns Gulch	07/18/1999	4.3	270	4,110	376	53	940	138	N.A.
South of Imogene Mine	09/15/1999	6.86	210	18	5	7	258	70.3	24.8
West of Imogene Mine	09/15/1999	7.44	182	30	5	8	34	73.2	N.A.
Southeast of Chattanooga	09/15/1999	6.51	314	230	35	10	143	130	N.A.
Big Horn Gulch	09/17/1999	6.92	125	80	214	24	317	31.50	22
East of Carbon Lake	09/17/1999	3.54	304	1,250	6,860	2,630	3,590	102	0.01
<u>Upper Animas River basin</u>									
Boulder Gulch	9/26/1997	7.45	93	63	10	4	25	22	21.5
Arrastra Creek	9/14/1997	7.92	184	41	7	3	147	44	41.5
Hematite Gulch	9/23/1998	8.24	277	55	30	4	20	81	59
California Gulch	8/18/1998	5.32	278	1,800	113	8	1,440	117	4
Blair Gulch	9/14/1997	7.52	673	30	10	1	776	360	50
Niagra Gulch	9/09/1988	7.27	195	40	30	4	20	61	35
Swansea Gulch	9/10/1991	6.9	92	N.A.	24	N.A.	76	N.A.	N.A.
Eureka Gulch	9/14/1998	7.1	308	140	30	6	373	117	22
Picayune Gulch	9/09/1998	6.86	386	62	30	4	20	127	69
Placer Gulch	9/28/1998	5.93	195	362	704	21	1,210	78	3
Idaho Gulch	6/25/1992	8.10	N.A.	20	15	9	50	N.A.	N.A.
Kendall Gulch	8/17/1998	7.82	129	15	5	8	8	12	N.A.

Values in italics are ½ detection limit

Red OFR-00-53, blue USGS Professional Paper 1651 database (2007), green Unpublished Report to Water Quality Control Commission, Animas River Stakeholders Group, 2001 Placer gulch sample UA33 is downstream of Evening Star Mine (mid-basin). SpC specific conductance

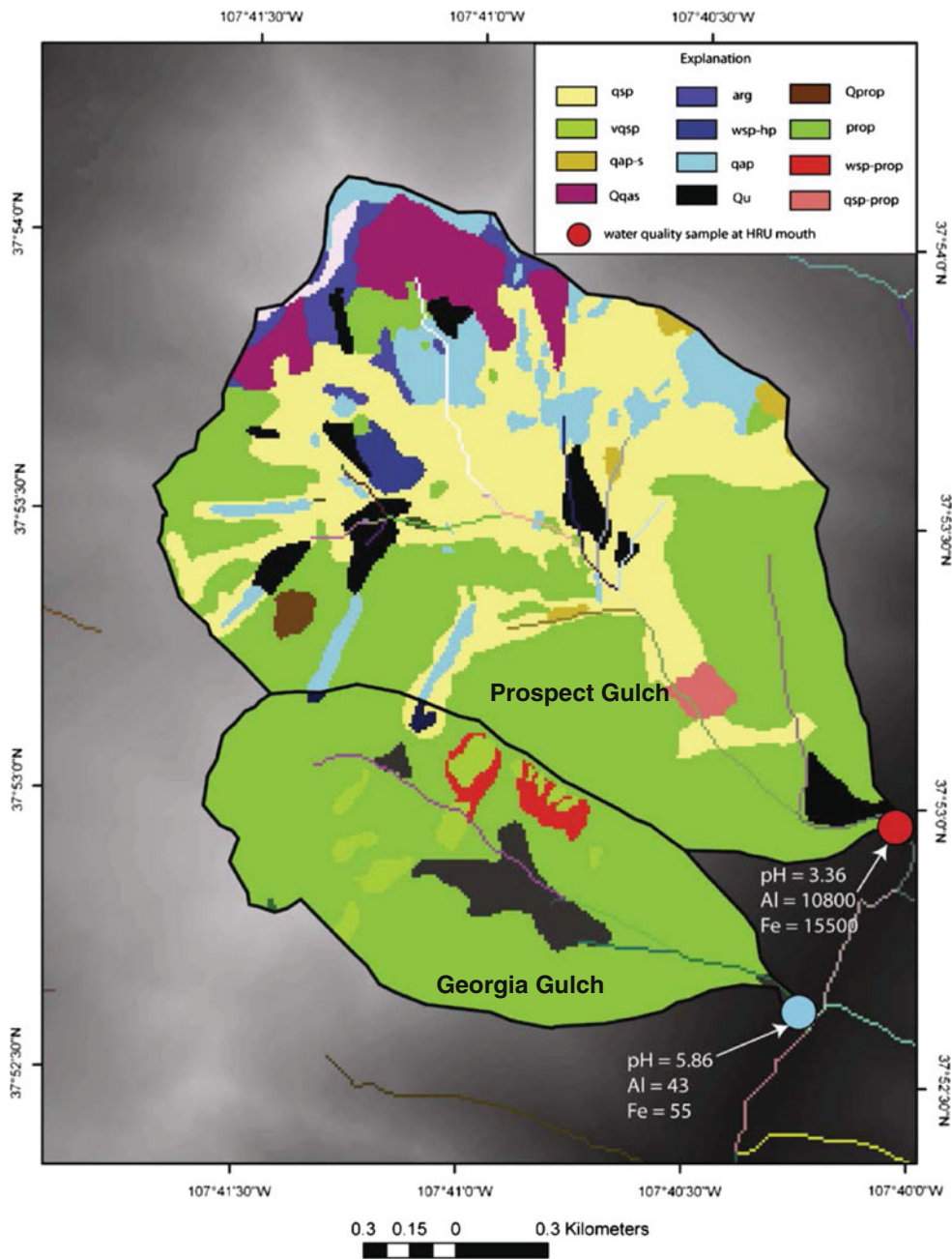


Fig. 6 Example of water quality samples collected at watershed outlets; parameters pH, Al, and Fe concentration shown for comparison. Watersheds have greatly differing proportions of alteration types with Georgia Gulch having much less acidic conditions due to the

presence of abundant propylitic rocks (*green*), and lower Al and Fe concentrations compared to Prospect Gulch. Detailed descriptions of alteration types in Bove et al. (2007a)

Areas of net acid production and effect on pH

Watershed NAP area calculations completed using the hybrid AVIRIS- and field-based alteration maps enabled comparisons between the sum of all NAP alteration types and pH. These data are useful for determining where acidic conditions are likely to occur. Acidic watersheds were not surprisingly found to have relatively high proportions of

NAP alteration. The NAP area determined for 17 acidic watersheds with pH < 5.5 ranges from 2.4 to 96.0 % with a mean NAP area of 46 %. Acidic watersheds having small areas of NAP alteration are commonly impacted by mining features such as draining adits. For example, GIS analysis of North Fork Cement Creek and East of Carbon Lakes watersheds with highly acidic water quality lacked significant NAP alteration and thus by inference could be

identified as being mining impacted (Table 2). In contrast, the NAP area for 29 watersheds with $\text{pH} > 5.5$ ranges from 0 to 24 % with a mean NAP area of only 4.1 %. Note that alteration assemblages containing mixtures of NAP and ANC, e.g., qsp-prop are included in the NAP area determinations. This is because the propylitic component may be insufficient to neutralize acidity attributed to weathering of the qsp component having $\text{NAP} > \text{ANC}$.

The Mineral Creek, Cement Creek, and upper Animas River basins have varying proportions of NAP rocks that are associated with multiple types of hydrothermal systems. The Mineral Creek basin in the western part of the study area is associated with (1) a low-grade Cu–Mo porphyry system that formed between South and Middle Forks of Mineral Creek and (2) with acid sulfate alteration centered on Ohio Peak–Anvil Mountain (OPAM) to the east (Bove et al. 2007a). Alteration associated with the Cu–Mo porphyry and acid sulfate systems is extensive with some watersheds in these areas being entirely and intensely altered. The Upper Cement Creek basin has significant areas of acid sulfate alteration within the Red Mountain mining district and is also impacted by alteration in the OPAM area that forms the drainage divide between Mineral and Cement Creek basins. Smaller areas of NAP alteration occur along vein structures of the Eureka graben. Alteration in the upper Animas River basin east of Silverton is mainly associated with caldera-related vein structures that formed in the South Silverton mining area and along the Eureka graben in California and Placer Gulch's (Varnes 1963; Casadevall and Ohmoto 1977).

Areas and watershed elevation of ANC rocks and effect on pH

Propylitic alteration containing abundant secondary ANC minerals (calcite, chlorite, epidote) is pervasive, overprinting most of the igneous sequence (Burbank 1960; Bove et al. 2007a). Propylitic alteration was mapped in 67 % of the study area. Regionally, extensive propylitic alteration is preserved where it is not overprinted by more intense hydrothermal alteration having NAP and affecting 9 % of the study area (Fig. 7; Table 4).

GIS calculations were used to determine the percent area and mean elevation of propylitic rocks in each watershed. If propylitic rocks are exposed in a watershed at a high elevation relative to the mean watershed elevation, weathering of these rocks could produce surface water with initial alkalinity that might mitigate acidity caused by weathering of NAP alteration or mining areas exposed at lower elevations. The percent area of propylitic rocks was also calculated for watersheds having greater and less than $\text{pH} 5.5$ at watershed outlets (Table 5). A pH of 5.5, similar to that of rainwater, was used as a gage for acidic versus less acidic water quality. Watersheds with less acidic to neutral water quality ($\text{pH} > 5.5$) have an average of 74 % propylitic area (Fig. 8). Only three of the less acidic to neutral watersheds (Big Horn, Placer, and Porcupine watersheds) have a mean elevation of propylitic rocks that is lower than the mean watershed elevation. In contrast, acidic watersheds average 44 % propylitic area and 64 % of those watersheds have a mean propylitic rock elevation that occurs below the watershed mean elevation (Fig. 8).

Fig. 7 Intensely altered propylitic rocks (*red and yellow*) in the Red Mountain mining district, overprinting the regional, propylitically altered igneous rocks (*grayish-green*), peaks at top of image. View to west



Table 4 Summary statistics determined by GIS for generalized propylitic rocks and net acid producing assemblages for (A) whole study area, and major basins; (B) watersheds that comprise each basin

	Propylitic area (%)	Net acid producing rocks (%)	pH
A			
Generalized alteration groups (whole watershed)	67	9	5.82
Generalized alteration types for basins			
Upper Animas River basin	77	3	7.12
Cement Creek basin	62	20	3.56
Mineral Creek basin	51	30	6.29
B			
Generalized alteration groups summary statistics for watersheds analyzed in each basin			
Upper Animas River	72	3	
Cement Creek basin	66	13	
Mineral Creek basin	53	25	

pH was determined on September 8, 2009 at hydrologic gage stations; whole study area pH represented by water quality sample collected near gage A72 below Silverton, Colorado

Mining impacts can overwhelm the ANC properties of propylitically altered rocks. For example, Mineral and Cement Creek basins have acidic surface water quality with Cement Creek being more acidic, despite Cement Creek basin having 11 % greater area of propylitic rocks (Table 4). Cement Creek is heavily impacted by mining compared with the less heavily mined Mineral Creek basin, and this could explain the lower pH of Cement Creek. In contrast to the more highly altered Mineral and Cement Creek basins, the upper Animas River basin on the western margin of the study area has low acidity, an average of 77 % propylitic rocks and only 3 % NAP rocks. The upper Animas River basin water sampled near the basin outlet upstream from Cement Creek has a near neutral pH (Table 4).

Vegetated and non-vegetated areas

Vegetated and non-vegetated areas were delineated using GIS analysis of AVIRIS-derived maps (Dalton et al. 2007). Alteration and vegetation layers were overlain to determine non-vegetated areas that intersect hydrothermally altered rock. Non-vegetated areas enhance the potential for erosion because plants are unavailable for interception of precipitation. Lack of interception by plants enhances splash detachment, an important physical weathering mechanism (Kinnell 2005). Intensely altered areas lacking vegetation tend to have more highly acidic water quality compared with vegetated areas. Acidic watersheds have an average of nearly 13 % non-vegetated areas that intersect NAP

alteration. In contrast, less acidic to neutral watersheds (pH > 5.5) have an average of 2 % non-vegetated areas that coincide with NAP alteration.

Morphometric parameters determined by GIS

The principal morphometric parameters that were statistically analyzed in relation to water quality signatures were basin area, stream length, and drainage density (Table 2, ESM only). These parameters are very similar for Mineral and Cement Creek basins. Upper Animas River basin watersheds are 26 % larger, have average stream lengths that are 32–37 % longer, and drainage densities that are nearly 8 % greater compared to Mineral and Cement Creek basins.

Slope and aspect were also considered to be potentially important morphometric parameters. Topographic relief in the study area is high and average watershed slopes are consistently steep with a gradient commonly >25°. This resulted in the slope showing no significant correlation with water quality. Additional data are needed to fully evaluate the role that aspect may play in influencing water quality. This is because aspect strongly controls the timing of snow melt runoff and thus influences when infiltration of surface water into soils and bedrock and subsequent weathering reactions occur. Southerly facing slopes, for example, experience earlier melting compared to northerly slopes, and snow lasts longer throughout a season on north facing slopes. To permit interpretations regarding potential effect on water quality signatures, data acquisition is required at different times during a hydrologic cycle for watersheds with similar proportions of alteration and with varying aspect.

Linear regression analysis of alteration data

TM data

Linear regression coefficients were determined for alteration assemblages mapped by analysis of TM data and water quality parameters for the combined, mined and unmined watersheds, and separately for watersheds having minimal mining impacts (Table 6). Despite only 2–3 % watershed areas being mapped by TM due to vegetation cover, statistically significant correlations were determined between TM-derived alteration types and water quality signatures. Negative correlations are observed between area of clay–sulfate–sericite¹ alteration (TM–CSM), pH,

¹ It is emphasized here that the TM-CSM is not mapping marble in the study area, but marble is permissive in this TM grouping defined by Rockwell (2010). The principal mineral groups mapped in hydrothermally altered areas include clays, sulfate (alunite), and sericite.

Table 5 Mean watershed elevation, mean elevation of propylitic rocks, total area of propylitic rocks, and pH for each watershed

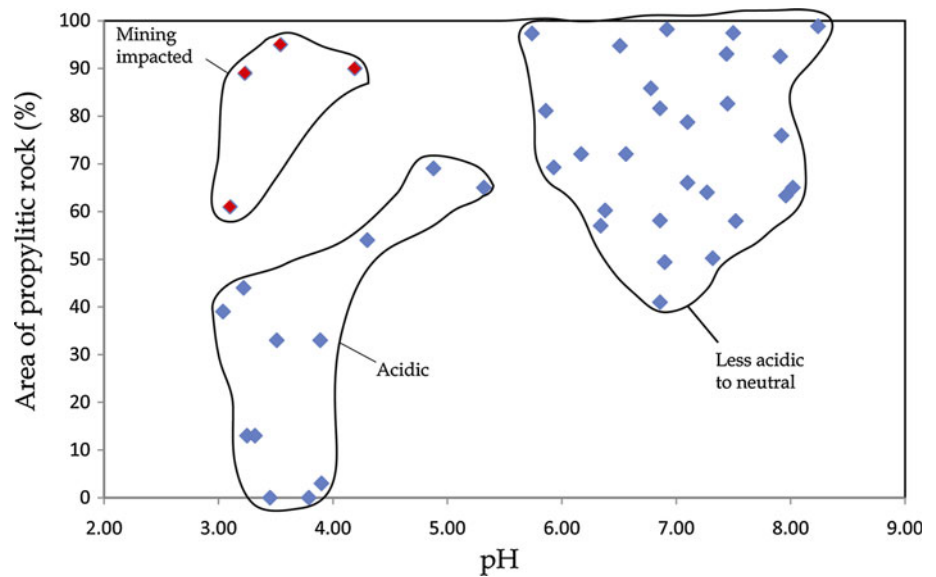
Watershed	Mean watershed elevation (m)	Mean elevation of propylitic rocks (m)	Pr propylitic rock area (%)	pH
Ohio Gulch	3,407	3,318	39	3.04
North Fork Cement	3,669	3,690	61	3.10
Prospect Gulch	3,551	3,503	44	3.22
Tiger Gulch	3,489	3,483	89	3.23
South of Browns Gulch	3,474	3,395	13	3.25
Red Tributary	3,524	3,576	13	3.32
South of Bonner	3,321	No propylitic	0	3.45
Niagra, Cement Creek Basin	3,441	3,300	33	3.51
East of Carbon Lake	3,517	3,516	95	3.54
Battleship Slide	3,395	No propylitic	0	3.79
Dry Gulch	3,562	3,451	33	3.89
Zuni Gulch	3,461	3,641	3	3.9
Minnesota	3,497	3,501	90	4.19
Browns Gulch	3,527	3,592	54	4.3
Topeka Gulch	3,401	3,370	69	4.88
California Gulch	3,758	3,736	65	5.32
<i>South of Dry</i>	3,453	3,459	97	5.74
Georgia	3,557	3,566	81	5.86
Placer	3,764	3,756	69	5.93
Ross	3,806	3,824	72	6.17
South Fork Cement	3,605	3,660	57	6.34
Porcupine	3,459	3,407	60	6.38
S.E. of Chattanooga	3,579	3,592	95	6.51
Middle Fork Central	3,504	3,585	72	6.56
Middle Fork East	3,437	3,471	86	6.78
South of Imogene	3,629	3,639	58	6.86
Paradise basin	3,639	3,714	41	6.86
Picayune Gulch	3,700	3,727	82	6.86
Swansea	3,545	3,625	49	6.90
<i>Big Horn</i>	3,612	3,609	98	6.92
<i>N.E. of Belcher</i>	3,512	3,515	66	7.10
Eureka	3,664	3,697	79	7.10
Niagra, Animas River Basin	3,826	3,830	64	7.27
Hancock	3,567	3,743	50	7.32
<i>W. of Imogene</i>	3,467	3,488	93	7.44
Boulder	3,668	3,685	83	7.45
Fairview	3,575	3,583	97	7.50
Blair	3,551	3,636	58	7.52
Illinois	3,555	3,583	97	7.50
<i>Arrastra</i>	3,595	3,697	76	7.92
Cascade	3,613	3,623	63	7.96
Middle Fork West	3,663	3,683	65	8.02
Hematite	3,678	3,686	99	8.24

Bold indicates elevation of propylitic rocks is higher than the mean watershed elevation, italics are watersheds with nearly equal mean elevation and propylitic mean elevation, non-italics and non-bold indicates mean elevation of propylitic rocks is lower than mean elevation

and alkalinity. Aluminum is positively correlated with area of TM–CSM. Area of iron alteration (TM–Fe) is negatively correlated with pH and alkalinity.

Unmined watersheds were analyzed separately to determine if correlations exist when mining impacts are excluded. Mining impacts, especially draining mine adits

Fig. 8 Propylitic alteration area (% of total watershed area) versus pH. Acidic watersheds average 44 % propylitic rock; less acidic to near neutral watersheds average 74 % propylitic rock. Mining impacted watersheds are clearly delineated by watersheds having abundant propylitic rock, yet having low pH



that are observed at several mining areas in Colorado, can adversely impact water quality and complicate interpretation of the geochemical background signal attributed to natural weathering processes of hydrothermally altered areas (Yager et al. 2010). In general, an increase in correlation values was observed when mined watersheds were excluded from regression analysis (Table 7). TM–CSM showed significant trends with pH, Fe (which were not observed in the combined mined and unmined dataset), Al, and alkalinity. Correlation values between TM–Fe, pH, Fe, Al, and Cu also increased. Alkalinity had a lower, negative correlation value compared with the combined mined and unmined dataset.

ASTER data

Alteration types mapped by ASTER and area calculations determined by GIS and used in statistical analysis are in Table 6. Two alteration assemblages, argillic plus ferric iron (Aster–Arg–Fe) and quartz–sericite–pyrite–phyllic (Aster–qsp), were observed to have correlations with water quality parameters. All argillic and qsp alteration types were also separately summed and statistically analyzed to evaluate the cumulative effect that the \sum all NAP assemblages have on water quality.

Aster–Arg–Fe is negatively correlated with pH and alkalinity. The major metal cations Fe, Al, and the trace metal Cu are positively correlated with area of Aster–Arg–Fe alteration, with aluminum having the the highest correlation. Analysis of the \sum all argillic alteration assemblages showed a similar trend compared to the Aster–Arg–Fe data, but had a slightly lower negative correlation with alkalinity. Area of Aster–qsp alteration is negatively correlated with pH and positively correlated

with Fe, Al, and Cu. Correlation values are higher for the \sum all qsp-bearing assemblages and the elements Fe, Al, and Cu, when compared to correlations obtained with the Aster–qsp alteration assemblage. The “propylitic or carbonate rock” assemblage is not significantly correlated with any water quality parameter.

Correlation values were generally higher for area of Aster–Arg–Fe and water quality parameters when mined watersheds were excluded from analysis (Table 7). This is especially true for pH, Fe, Al, and Cu; however, the negative correlation value for alkalinity observed in the combined mined and unmined dataset decreased for the unmined dataset. Correlations also increased for area of Aster–qsp and water quality parameters pH, Fe, and Al when mined watersheds were excluded. Correlation values for the \sum all qsp alteration assemblages in unmined watersheds yielded a lower correlation value with pH and a positive correlation with Fe, Al, and Cu that are similar compared to the dataset that includes both mined and unmined watersheds. The propylitic or carbonate rock assemblage showed no statistically significant trends with water quality parameters when mined catchments were excluded.

Hybrid AVIRIS and field mapping data

Significant correlation values are observed for three acid-generating alteration types (arg, qsp, and qap) mapped by hybrid AVIRIS- and field-based data (Table 6). In addition, correlations are observed between the \sum all NAP, the ratio \sum propylitic: \sum all NAP, and water quality. Aluminum is positively correlated with area of argillic alteration. No additional water quality parameters are correlated with argillic alteration. Quartz–sericite–pyrite has a relatively high negative correlation with pH, and positive correlation

Table 6 Linear regression coefficients for area of alteration types determined using TM, ASTER, hybrid AVIRIS and field mapping data, and water quality parameters for combined mined and unmined watersheds

Alteration type	pH	Fe	Al	Cu	Zn	SO ₄	Alkalinity	Specific conductance
TM								
Clay–sulfate–sericite alteration	-0.32 (0.03) <i>N</i> = 24	0.27 (0.05) <i>N</i> = 24	0.41 (0.005) <i>N</i> = 24	0.19 (0.19) <i>N</i> = 25	0.11 (0.45) <i>N</i> = 24	0.29 (0.05) <i>N</i> = 24	-0.56 (0.02) <i>N</i> = 12	
Iron alteration	-0.38 (0.0001) <i>N</i> = 34	0.38 (0.001) <i>N</i> = 33	0.43 (0.0004) <i>N</i> = 33	0.38 (0.002) <i>N</i> = 32	0.35 (0.45) <i>N</i> = 24	0.29 (0.004) <i>N</i> = 33	-0.51 (0.002) <i>N</i> = 20	
ASTER								
∑ of all argillic alteration	-0.37 (0.0009) <i>N</i> = 38	0.41 (0.0002) <i>N</i> = 37	0.47 (0.00003) <i>N</i> = 39	0.39 (0.0004) <i>N</i> = 37	0.16 (0.14) <i>N</i> = 38	0.07 (0.51) <i>N</i> = 38	-0.32 (0.03) <i>N</i> = 23	
Argillic plus ferric iron alteration	-0.38 (0.001) <i>N</i> = 35	0.39 (0.0009) <i>N</i> = 35	0.44 (0.0002) <i>N</i> = 35	0.41 (0.0005) <i>N</i> = 35	0.15 (0.19) <i>N</i> = 35	0.14 (0.23) <i>N</i> = 35	-0.46 (0.006) <i>N</i> = 19	
Quartz–sericite–pyrite (phyllic)	-0.42 (0.002) <i>N</i> = 27	0.39 (0.004) <i>N</i> = 26	0.45 (0.0009) <i>N</i> = 28	0.32 (0.01) <i>N</i> = 27	0.18 (0.2) <i>N</i> = 27	0.16 (0.27) <i>N</i> = 26	-0.18 (0.44) <i>N</i> = 12	
∑ of all Quartz–sericite–pyrite alteration	-0.41 (0.0006) <i>N</i> = 34	0.47 (0.00007) <i>N</i> = 32	0.55 (0.00005) <i>N</i> = 33	0.42 (0.00004) <i>N</i> = 34	0.12 (0.3) <i>N</i> = 34	0.15 (0.22) <i>N</i> = 33	-0.16 (0.34) <i>N</i> = 19	
Propylitic or carbonate rocks	0.24 (0.07) <i>N</i> = 28	-0.17 (0.2) <i>N</i> = 27	-0.08 (0.57) <i>N</i> = 28	-0.28 (0.03) <i>N</i> = 28	0.01 (0.9) <i>N</i> = 28	0 (1) <i>N</i> = 27	0.06 (0.71) <i>N</i> = 21	
AVIRIS								
Argillic alteration	-0.25 (0.24) <i>N</i> = 13	0.28 (0.28) <i>N</i> = 13	0.46 (0.03) <i>N</i> = 13	0.31 (0.16) <i>N</i> = 13	-0.23 (0.29) <i>N</i> = 13	0.31 (0.16) <i>N</i> = 13	-0.04 (1) <i>N</i> = 7	0.28 0.20 <i>N</i> = 13
Quartz–sericite–pyrite alteration	-0.52 (0.003) <i>N</i> = 18	0.52 (0.003) <i>N</i> = 18	0.62 (0.0003) <i>N</i> = 18	0.34 (0.05) <i>N</i> = 18	0.18 (0.32) <i>N</i> = 18	0.23 (0.1) <i>N</i> = 18	-0.43 (0.17) <i>N</i> = 8	0.29 0.09 <i>N</i> = 18
Quartz–alunite–pyrophyllitic alteration	-0.49 (0.003) <i>N</i> = 12	0.15 (0.54) <i>N</i> = 12	0.36 (0.11) <i>N</i> = 12	0.12 (0.63) <i>N</i> = 12	0.21 (0.37) <i>N</i> = 12	0.06 (0.83) <i>N</i> = 12	-0.33 (0.45) <i>N</i> = 6	0.06 0.84 <i>N</i> = 12
∑ of NAP alteration	-0.41 (0.002) <i>N</i> = 28	0.29 (0.03) <i>N</i> = 28	0.39 (0.004) <i>N</i> = 28	0.19 (0.16) <i>N</i> = 28	0.14 (0.28) <i>N</i> = 28	0.28 (0.04) <i>N</i> = 28	-0.28 (0.09) <i>N</i> = 19	0.30 0.02 <i>N</i> = 28
∑ of propylitic alteration:∑NAP alteration (ratio)	0.46 (0.0009) <i>N</i> = 26	-0.29 (0.03) <i>N</i> = 26	-0.38 (0.009) <i>N</i> = 26	-0.18 (0.20) <i>N</i> = 25	0.02 (0.88) <i>N</i> = 26	-0.16 (0.26) <i>N</i> = 25	0.44 (0.09) <i>N</i> = 18	-0.19 0.17 <i>N</i> = 26

Values in bold indicate statistical trends

P values are in parenthesis, *N* is number of watersheds used in analyses

with Fe and Al. A possible positive trend is observed between qsp and Cu. Quartz–alunite–pyrophyllite is negatively correlated with pH, but lacks additional correlations with other water quality parameters. The ∑all NAP alteration is negatively correlated with pH, positively

correlated with Al, and yields weaker positive trends with Fe, specific conductance, and SO₄. A positive trend is also observed for the ratio ∑propylitic:∑all NAP and pH.

Selected morphometric parameters are correlative with the area of propylitically altered bedrock. A positive

Table 7 Linear regression coefficients for area of alteration types determined using TM, ASTER and hybrid AVIRIS and field mapping data and water quality parameters for unmined watersheds

Remote sensing platform and alteration type	pH	Fe	Al	Cu	Zn	SO ₄	Alkalinity	Specific conductance
TM								
Clay–sulfate–sericite alteration	-0.47 (0.02) <i>N</i> = 15	0.47 (0.02) <i>N</i> = 15	0.46 (0.02) <i>N</i> = 15	0.33 (0.09) <i>N</i> = 15	0.05 (0.8) <i>N</i> = 15	0.22 (0.27) <i>N</i> = 15	-0.62 (0.07) <i>N</i> = 7	
Iron alteration (unmined)	-0.57 (0.0002) <i>N</i> = 22	0.51 (0.0009) <i>N</i> = 21	0.52 (0.0009) <i>N</i> = 21	0.45 (0.004) <i>N</i> = 20	0.25 (0.11) <i>N</i> = 21	0.22 (0.16) <i>N</i> = 21	-0.45 (0.03) <i>N</i> = 14	
ASTER								
∑ of all argillic alteration	-0.43 (0.002) <i>N</i> = 26	0.47 (0.0006) <i>N</i> = 25	0.58 (0.00003) <i>N</i> = 26	0.45 (0.0008) <i>N</i> = 25	0.25 (0.06) <i>N</i> = 25	-0.02 (0.89) <i>N</i> = 26	-0.26 (0.15) <i>N</i> = 17	
Argillic plus ferric iron alteration	-0.47 (0.002) <i>N</i> = 23	0.47 (0.0002) <i>N</i> = 23	0.56 0.0002 <i>N</i> = 23	0.49 (0.001) <i>N</i> = 23	0.19 (0.19) <i>N</i> = 23	0.04 (0.79) <i>N</i> = 23	-0.39 (0.05) <i>N</i> = 14	
Quartz–sericite–pyrite (phyllic)	-0.50 (0.004) <i>N</i> = 18	0.54 (0.002) <i>N</i> = 18	0.60 (0.0005) <i>N</i> = 18	0.47 (0.006) <i>N</i> = 18	0.29 (0.09) <i>N</i> = 18	0.11 (0.52) <i>N</i> = 18	-0.08 (0.83) <i>N</i> = 8	
∑ of all Quartz–sericite–pyrite alteration	-0.33 (0.03) <i>N</i> = 23	0.49 (0.001) <i>N</i> = 21	0.59 (0.000007) <i>N</i> = 22	0.46 (0.002) <i>N</i> = 23	0.07 (0.3) <i>N</i> = 23	0.02 (0.89) <i>N</i> = 23	-0.04 (0.87) <i>N</i> = 14	
Propylitic or carbonate rocks	0.23 (0.18) <i>N</i> = 19	-0.05 (0.75) <i>N</i> = 18	-0.04 (0.83) <i>N</i> = 19	-0.34 (0.04) <i>N</i> = 19	0.07 (0.69) <i>N</i> = 19	0.04 (0.8) <i>N</i> = 19	0.08 (0.69) <i>N</i> = 15	
AVIRIS								
Quartz–sericite–pyrite alteration	-0.45 (0.05) <i>N</i> = 12	0.48 (0.03) <i>N</i> = 12	0.66 0.003 <i>N</i> = 12	0.35 (0.13) <i>N</i> = 12	0.03 (0.94) <i>N</i> = 12	0.24 (0.31) <i>N</i> = 12	-0.6 (0.22) <i>N</i> = 5	0.33 0.14 <i>N</i> = 12
Quartz–alunite–pyropropylitic alteration	-0.52 (0.13) <i>N</i> = 7	0.14 (0.76) <i>N</i> = 7	0.52 (0.13) <i>N</i> = 7	0.14 (0.76) <i>N</i> = 7	-0.14 (0.76) <i>N</i> = 7	0.04 (1) <i>N</i> = 7	-0.66 (0.30) <i>N</i> = 4	0.14 0.76 <i>N</i> = 7
∑ of all NAP alteration	-0.66 (0.0002) <i>N</i> = 17	0.49 (0.006) <i>N</i> = 17	0.54 0.0004 <i>N</i> = 16	0.42 (0.03) <i>N</i> = 16	0.23 (0.21) <i>N</i> = 17	0.5 (0.008) <i>N</i> = 16	-0.63 (0.008) <i>N</i> = 11	0.45 0.01 <i>N</i> = 17
∑ of propylitic alteration:∑ of all NAP alteration (ratio)	0.63 (0.0001) <i>N</i> = 15	-0.42 (0.03) <i>N</i> = 15	-0.53 (0.010) <i>N</i> = 14	-0.34 (0.10) <i>N</i> = 14	0.13 (0.52) <i>N</i> = 15	-0.34 (0.10) <i>N</i> = 14	0.64 (0.01) <i>N</i> = 10	-0.28 0.16 <i>N</i> = 15

Values in bold indicate statistical trends

P values are in parenthesis, *N* is number of watersheds used in analyses

regression value ($R = 0.63, n = 40$) is observed between area of propylitic rocks and total watershed area. Positive trends are also observed between area of propylitic alteration, stream length ($R = 0.31, n = 40$), and non-vegetated area ($R = 0.66, n = 40$).

Exclusion of mined watersheds resulted in very similar trends between area of qsp alteration, pH, Fe, and Al when compared with the dataset containing mined and unmined

watersheds (Table 7). The largest increase in regression values in the unmined dataset was observed for both the ∑all NAP alteration types and the ratio of propylitic to NAP alteration and water quality. The ∑all NAP areas have a negative correlation with pH and alkalinity. Positive correlations were also observed for the ∑all NAP areas, and Fe, Al, Cu, specific conductance, and sulfate. The ratio ∑propylitic:∑all NAP resulted in positive correlations

Table 8 Linear regression coefficients for 30 m GIS stream buffered area intersecting alteration type and water quality parameters for mined and unmined watersheds

Buffer alteration type	pH	Fe	Al	Cu	Zn	Specific conductance	SO ₄	Alkalinity
Quartz–sericite–pyrite alteration buffer	-0.40 (0.05) <i>N</i> = 14	0.25 (0.23) <i>N</i> = 14	0.36 (0.08) <i>N</i> = 14	0.48 (0.01) <i>N</i> = 14	-0.12 (0.58) <i>N</i> = 14	0.03 0.91 <i>N</i> = 14	0.03 (0.91) <i>N</i> = 14	-0.73 (0.06) <i>N</i> = 6
∑of non propylitic alteration buffer	-0.42 (0.007) <i>N</i> = 21	0.32 (0.04) <i>N</i> = 21	0.49 0.002 <i>N</i> = 21	0.21 (0.17) <i>N</i> = 21	0.09 (0.58) <i>N</i> = 21	0.18 0.25 <i>N</i> = 21	0.09 (0.59) <i>N</i> = 21	-0.17 (0.50) <i>N</i> = 12
Propylitic alteration buffer	0.17 (0.12) <i>N</i> = 39	-0.07 (0.50) <i>N</i> = 39	-0.01 (0.90) <i>N</i> = 39	-0.02 (0.83) <i>N</i> = 39	0.09 (0.42) <i>N</i> = 39	-0.05 0.65 <i>N</i> = 39	-0.11 (0.33) <i>N</i> = 39	0.14 (0.30) <i>N</i> = 28

GIS stream buffer was applied to hybrid, AVIRIS and field mapping data

Values in bold indicate statistical trends

P values are in parenthesis, *N* is number of watersheds used in analyses

Table 9 Linear regression coefficients for 30 m GIS stream buffered area intersecting alteration type and water quality parameters for unmined watersheds

Buffer alteration type	pH	Fe	Al	Cu	Zn	Specific conductance	SO ₄	Alkalinity
∑of non propylitic alteration buffer	-0.48 (0.03) <i>N</i> = 12	0.45 (0.05) <i>N</i> = 12	0.67 0.003 <i>N</i> = 12	0.38 (0.09) <i>N</i> = 12	0.12 (0.63) <i>N</i> = 12	0.36 0.11 <i>N</i> = 12	0.24 (0.30) <i>N</i> = 12	-0.73 (0.06) <i>N</i> = 6

GIS stream buffer was applied to hybrid, AVIRIS and field mapping data

Values in bold indicate statistical trends

P values are in parenthesis, *N* is number of watersheds used in analyses

with pH and alkalinity. Fe and Al are negatively correlated with area of propylitically altered bedrock. Exclusion of mined watersheds does not increase the strength of morphometric correlations observed with area of propylitic alteration.

Area of vegetation

Correlations between non-vegetated and whole watershed areas of qsp alteration and water quality parameters were similar, both having negative correlations with pH ($R = -0.41$, $n = 19$) and positive correlations with Fe ($R = 0.36$, $n = 19$) and Al ($R = 0.56$, $n = 19$). Area of non-vegetated qap is negatively correlated with pH ($R = -0.51$, $n = 12$) and has a similar negative correlation value that is also observed for whole watershed area of qap alteration.

Hybrid AVIRIS and field mapping data (30-m GIS stream-buffered area analysis)

Linear regression analysis was performed on the intersected area of alteration types along a 30-m GIS stream buffer and water quality signatures. Area statistics for

GIS-buffered areas of qsp alteration is in Table 3 (ESM only). In general, the stream buffered area analysis yielded weaker correlations compared with the total watershed area. Buffered area of qsp alteration is negatively correlated with pH (Table 8). Copper is also more highly correlated with GIS-buffered areas of qsp compared with whole watershed area analysis. Alkalinity is negatively correlated with area of qsp, although the small sample size ($n = 6$) requires additional data to confirm this correlation. The sum of NAP alteration is negatively correlated with pH and is positively correlated with Al, with the regression value being higher for Al compared with whole watershed analysis. Correlations for Fe, Al, and alkalinity increased when mined watersheds were excluded from regression analysis (Table 9). GIS-buffered propylitic areas along streams are not correlative with either pH or alkalinity.

Factor analysis

TM data

A four factor model was used to explain 84 % of the variance for TM data with factors one and two accounting

for 60 % of the variance (Table 4, ESM only). Factor 1 loadings (29 % of the variance) indicate the highest correlation for areas of iron and clay–sulfate–sericite alteration. There is also a corresponding, weak inverse correlation with alkalinity that is likely caused by the increased weathering of hydrothermally altered areas and possible lack of propylitic rocks that have ANC. Factor 2 represents 26 % of the variance and has a weak negative correlation with the TM_Mod_Fe_2 classification defined by Rockwell (2010). Aluminum, Fe, SO_4 , and specific conductance all have inverse correlations with pH. Factor 2 loading scores are consistent with a correlation between increased area of iron alteration, corresponding low pH and an increase in major metal cations (Al and Fe), SO_4 , and specific conductance.

ASTER data

A six factor model was used to explain 92 % of the variance for the ASTER dataset, with factors one and two accounting for 56 % of the variance (Table 5, ESM only). Factor 1, with 33 % of variance indicates a strong, positive correlation for areas of clay, ferric iron, and qsp alteration. The high correlations for Al and Fe are consistent with weathering of hydrothermally altered rocks in watersheds having abundant aluminum-bearing clay minerals in addition to oxidation of pyrite and other sulfide phases. Weak correlations are observed for pH and specific conductance that would be expected in these more highly altered watersheds. Factor 2 represents 24 % of the variance and shows correlations between the multiple subtypes of propylitically altered rocks mapped by ASTER. There is no associated correlation, however, between propylitic rocks and pH. This finding could be a result of the limits of ASTER data in completely mapping a watershed because of vegetation cover that ultimately reduces the detectable area of propylitically altered bedrock having ANC. Factor 3 represents 12 % of the variance with the metals (Fe, and Al), SO_4 , and specific conductance being inversely correlated with pH. Factor 4 represents 10 % of the variance and shows correlations between pH, Cu, and Zn. Correlative Cu and Zn is consistent with weathering of a base metal sulfide mineral assemblage containing copper and zinc sulfides that are common in polymetallic veins in the study area.

The importance of the propylitic assemblage in mitigating ARD can be inferred in factor 5 (9 % of variance). Low pH and low alkalinity are correlated with watersheds having a relatively small area of propylitic alteration. Thus, minimal ANC is supplied by propylitically altered rocks to mitigate NAP. Factor 6, representing 5 % of the variance has a weak positive correlation with pH and a corresponding positive correlation with the mixed, regional propylitic to weak qsp and minor sericite assemblage.

Metal concentrations Al and Fe are also negatively correlated. This suggests that ANC and possible decreased metal abundances attributed to weathering of propylitically altered rocks as part of this mixed assemblage overwhelms any NAP produced by the weak qsp and minor sericite-bearing rocks.

Hybrid AVIRIS and field data

A six factor model was used to explain 80 % of the variance in the hybrid AVIRIS- and field-based dataset (Table 6, ESM only). Factor 1 represents 24 % of the variance and shows an inverse correlation between pH and the NAP alteration types argillic, qsp, gap, and $\sum \text{qsp} + \text{gap}$. Al, Fe, and Cu concentrations, sulfate and specific conductance are inversely correlated with pH. Factor 2 explains 24 % of the variance and identifies positive correlations among the morphometric parameters of stream length, total area, and propylitically altered rocks. In addition, both vegetated, non-vegetated areas, and area of quaternary deposits are all positively correlated. Weaker positive correlations are observed for wsp and \sum of all NAP. These patterns are consistent with large watersheds having an abundance of propylitically altered rocks and longer total stream lengths. Factor 3 explains 11 % of the variance. Variables that are correlated include the NAP alteration types qsp, $\sum \text{qsp} + \text{gap}$, wsp-hp and Zn. It is uncommon that Zn is correlated with alteration variables mapped by the TM and ASTER datasets. Thus, hybrid AVIRIS-field maps may be a more useful tool in identifying possible impacts to water quality from weathering of mineralized areas containing base metals. Factor 4 represents 8 % of the variance and shows correlations between sulfate and specific conductance. Factor 5, representing 8 % of the variance shows correlations between the ratio $\sum \text{propylitic} : \sum \text{non-propylitic}$, pH, and alkalinity. No correlation is observed for only the area of propylitically altered rocks indicating that the ratio of ANC (propylitic) to NAP (non-propylitic) is the controlling factor in determining alkalinity and pH, and not just the area of ANC. Factor 6 consists of 6 % of the variance and indicates a positive correlation between drainage density and wsp-hyd alteration. Wsp-hyd alteration may be more prone to weathering that could cause an increase in drainage density compared with other alteration types that do not show a similar trend.

Discussion

GIS was valuable in quantifying areas of alteration derived from TM, ASTER, and hybrid AVIRIS-field mapping datasets. While it is useful to characterize the primary

igneous units that had formed prior to alteration, weathering of hydrothermally altered bedrock and associated mineral deposits is the primary cause of resultant water quality. This is because there are few igneous units in the study area that have not been altered to at least some degree, modifying the primary igneous minerals to a secondary alteration mineral assemblage. GIS analysis identified the study area as being comprised of 67 % propylitic ANC rocks that are overprinted by 6 % NAP rocks. The low NAP:ANC ratio is informative because it highlights that only a small proportion of NAP alteration is necessary to adversely impact water quality. Mining impacts that are usually coincident with areas of NAP alteration add to the acid and metal loads to surface water and groundwater. Where the NAP:ANC ratio is high, water quality impacts are severe that have toxic effects on aquatic life. Two basins with a high average NAP:ANC ratio are Mineral Creek and Cement Creek. Severe to acute Al, Cu, Zn, and Cd toxicity is observed for trout and sensitive taxa in the Mineral and Cement Creek basins (Besser et al. 2007). In contrast to areas that are pervasively altered to NAP assemblages, watersheds having mostly vein-related mineralization are characterized by alteration confined to narrow zones adjacent to veins that do not pervade adjacent propylitic rocks. The south Silverton mining area contains several watersheds with prevalent vein-related mineralization. GIS analysis delineates small areas of NAP alteration in the south Silverton mining area and large areas of propylitic alteration consistent with water quality having neutral pH, and low metal concentrations with the exception of Zn in some watersheds that can locally sustain trout (Besser et al. 2007).

The average elevation of propylitically altered rocks relative to the mean watershed elevation determined by GIS was found to be an important factor affecting water quality. Less acidic to neutral watersheds tend to have propylitically altered rocks that form at an average elevation that is higher than the mean watershed elevation. In contrast, the average elevation of propylitically altered rocks in acidic watersheds is usually lower than the mean watershed elevation. When propylitically altered rocks occur at high elevations in mountain watersheds where precipitation is commonly greater and snow melt is more persistent throughout the spring and summer, this provides a consistent source of alkalinity to help mitigate ARD.

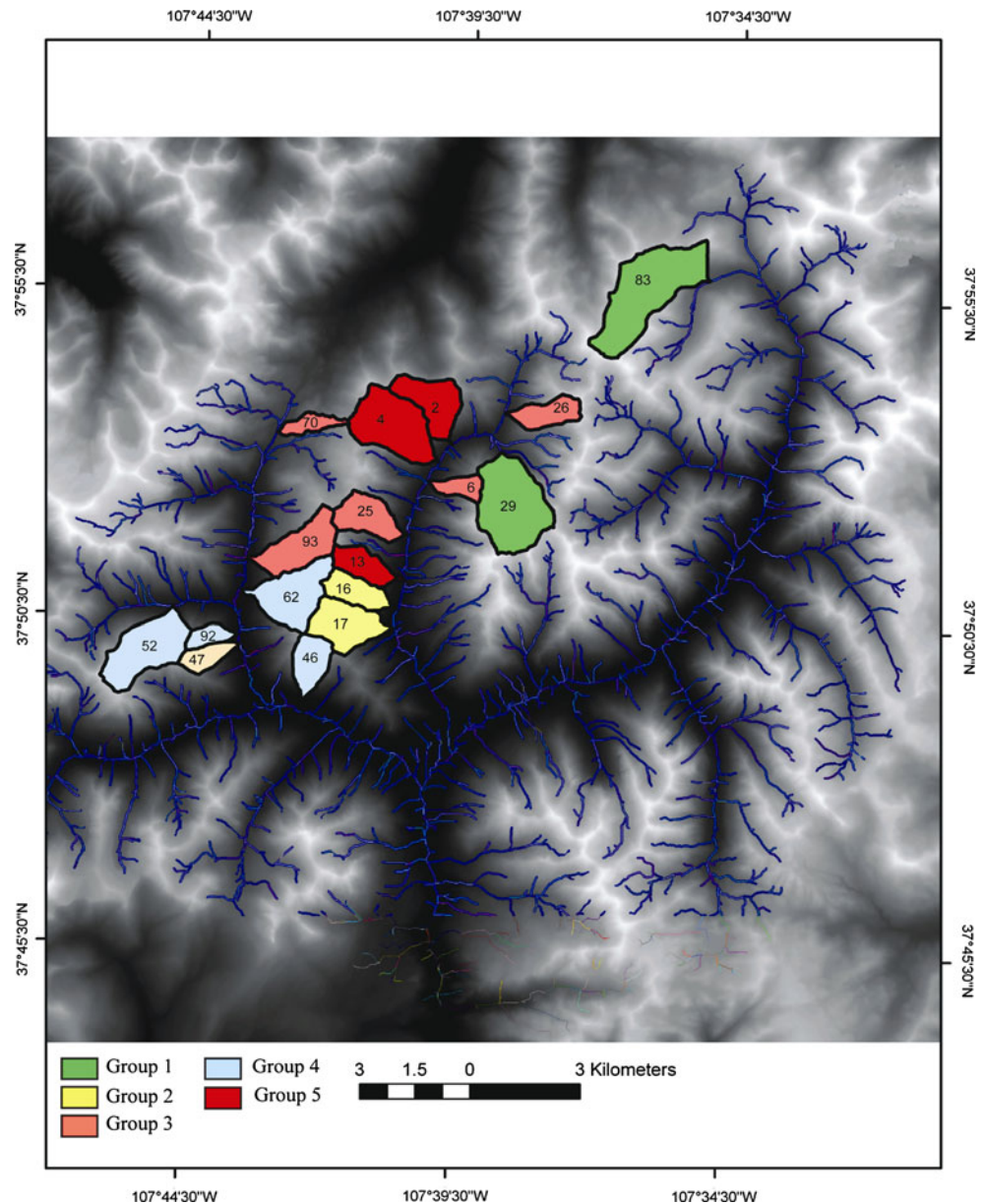
A watershed grouping schema was developed for mined and unmined watersheds using a limited numbers of variables including alteration type area determined using GIS analysis of AVIRIS data, surface water pH at watershed outlets, historical records, and field observations. Land managers could benefit from such a schema that would aid in quickly assessing watersheds in terms of possible geo-environmental impacts. This analysis used pH data because

it is a quickly acquired field parameter that can also be a proxy for other water quality impacts such as high metal and sulfate concentrations. Five watershed groupings were determined based on similarities in pH, area affected by NAP alteration, and mining impacts (Fig. 9). Group 1 watersheds may represent the best case scenario for possible reclamation success and mitigating mining impacts due to the large watershed size and low NAP:ANC ratio. In contrast, a high NAP:ANC ratio for group 5 watersheds may pose the greatest geo-environmental challenges due to acidic surface water conditions that existed prior to mining. Mining impacts for group 3 watersheds are clearly delineated due to the low NAP:ANC ratio, yet having acidic pH. Group 2 and 4 watersheds have minimal mining impacts and have acidic surface water quality because of varying proportions of NAP alteration. This type of grouping could aid in prioritizing reclamation resources for geo-environmental cleanup and also aid mining companies in identifying watershed NAP and ANC characteristics. Where information about specific mineral deposit types is also known, a prediction of the types of water quality impacts could be more completely discerned.

Statistical analysis in this study was effective in determining the association between watershed characteristics and water quality signatures. Previous preliminary studies also established correlations between water quality and areas of alteration mapped using the hybrid AVIRIS- and field-based data (Yager et al. 2008a, b). It was not known, however, whether less detailed alteration maps derived from TM and ASTER would also be effective in determining correlations with watershed properties. Analysis in this study revealed correlations with water quality parameters despite relatively small percentages of watershed areas being mapped by TM and ASTER alteration datasets because of vegetation cover. This has important implications for national geo-environmental and mineral assessments, especially in areas of the western United States that are more suitable to spectral mapping by remote sensing methods because the western regions are often not as highly vegetated as eastern US terrain.

Linear regression analysis identified correlations between mineral groups mapped by TM (TM–CSM, TM–Fe), major metal cations (Fe, Al) in surface water and low pH. These results were achieved despite a relatively small watershed area being mapped by TM. TM data are available for the entire US and suggest that when more detailed mineral maps are not available, TM could be useful in identifying potential water quality impacts from hydrothermally altered areas. ASTER was able to map a larger watershed area compared with TM and linear regression analysis revealed correlations between Aster–Arg–Fe, Aster–qsp, major metal cations (Fe, Al) in surface water and low pH. ASTER data are also available for the entire US and when

Fig. 9 Watersheds grouped based on percent NAP alteration area, mining impacts, and pH. Group 1 (*green*) have 10–20 % NAP area, are mining impacted, and pH ranging from 5.07 to 5.21; Group 2 (*yellow*) have 30–40 % NAP, have minimal mining impacts, and pH ranging from 3.58 to 4.88; Group 3 (*coral*) have <10 % NAP, are mining impacted, and pH ranging from 2.88 to 4.19; Group 4 (*light blue*) have 50–100 % NAP, have minimal mining impacts, and pH ranging from 3.45 to 3.90; Group 5 (*red*) have 50–85 % NAP, are mining impacted, and pH ranging from 3.04 to 3.89. Watershed id's correspond with those labeled in Fig. 2



more specific mineralogic data such as the presence of propylitic rocks containing acid neutralizing assemblages calcite and chlorite are required, ASTER can be used to augment mapping by TM. In general, correlations between NAP assemblages and water quality signatures are improved when mining impacted watersheds were excluded from analysis, suggesting that the GIS and statistical methods used in this study could be effective in unmined and hydrothermally altered areas to identify possible naturally occurring sources of acidity and metals to surface water.

AVIRIS mineral mapping have the most complete watershed area coverage and the highest correlations in regression analysis. The area of qsp was determined to

have the highest correlations with major metal cations (Fe, Al) and low pH. Quartz–alunite–pyrophyllite and argillic alteration types mapped by AVIRIS are each correlated with low pH. Argillic rocks are also correlated with aluminum. Correlations were also observed between increasing areas of propylitic rocks mapped by AVIRIS, watershed area, increasing pH and alkalinity. Similar correlations using propylitic bedrock mapping by ASTER were lacking that is likely due to the much smaller watershed area mapped by ASTER. This suggests that to understand the acid neutralizing capacity of a watershed, more complete watershed area mapping is required.

Statistical correlations are generally higher for whole watershed area analysis when compared to linear correlations

that involve analysis of altered areas intersected by a 30-m GIS stream buffer. In-stream processes were hypothesized as possibly being more important in controlling water quality signatures because of the effectiveness that the hydrologic stream network has in conveying sediment and associated contaminants to watershed outlets. In general, altered areas intersected by a GIS buffer were less highly correlated compared with alteration areas calculated for whole watersheds. This finding suggests that the whole watershed analysis is a better geochemical integrator of water quality signatures derived from weathering of hydrothermally altered areas. Most watersheds near Silverton, Colorado have steep slopes; therefore, physical and chemical weathering work to effectively transport sediment and simultaneously leach contaminants to streams throughout the entire area. A GIS stream buffer, if applied to a lower gradient region, may result in higher correlations with water quality signatures compared to steep terrain because downslope slumping and transport of sediment may be less important in rapidly conveying sediment to streams allowing for a greater water–sediment contact time.

Factor analysis allowed trace metal patterns to be identified that are consistent with weathering of sulfide-bearing hydrothermally altered areas. Only correlations between Cu and selected alteration assemblages were identified in linear regression analysis. Thus, correlations with other trace metals besides Cu in factor analysis is significant because it identified associated geochemical indicators that were predicted based on the mineral deposit types that are prevalent in the study area. An example of base metal correlations is observed for the ASTER data set in which Cu and Zn are inversely correlated with pH, reflecting increased trace metal abundances with acidic conditions. Patterns were also identified in factor analysis of AVIRIS data involving propylitically altered areas. In these analyses, the ratio ANC:NAP is correlated with pH and alkalinity, highlighting the importance of the relative proportions of acid neutralizing- and net acid producing-rocks in controlling acidity.

Conclusions

This analysis methodology emphasizes the importance of watersheds as key geographic units for interpreting water quality signatures in a geologic and morphometric context. Sampling strategies devised when a project is initiated could maximize the potential benefits of watershed scale analysis. Such a strategy would involve sampling watersheds of interest at the outlet during base flow conditions when concentrations of contaminants are not diluted by snowmelt or high precipitation. Analyses of watershed

outlet samples would provide integrated geochemical information for all up-stream contributing areas, and constituents measured would be a result of the water–soil–atmosphere interactions along the entire upstream flow path. Standard field parameters would be collected including pH, specific conductance, dissolved oxygen, alkalinity, in addition to metal cations, anions, and sulfate. Mapping of geology, alteration, vegetation, terrain, and delineation of the hydrologic network would permit each watershed or basin to be well characterized and subsequently analyzed with GIS tools. Resultant data for watershed physical characteristics compiled from GIS would provide a basis for statistical analysis. This methodology would likely be valuable, especially in unmined areas, because the information acquired would begin to establish a geochemical baseline that could be compared to data collected once mining began or ceased. This approach would also enable watersheds to be ranked as to potential geoenvironmental impacts prior to and after mining.

Future analysis requires that basin-scale (10 s to 100 km²) areas be analyzed using a GIS and statistical methodology similar to that used in this study. In order to upscale to larger areas, conservative geochemical constituents that are collected at basin outlets will need to be evaluated. Sulfate, pH, or major metal cations (Al and Fe) may provide the best evidence for large-scale impacts to water quality from hydrothermally altered and mineralized areas. Geochemical data determined for stream sediments collected as part of the National Uranium Resource Evaluation (NURE) or during USGS Bureau of Land Management mineral assessment studies may be useful datasets for up-scaling. The stream sediments, while not providing a direct link to water quality effects, may provide an indication of possible bioavailable elements that could potentially impact water quality and aquatic life.

Acknowledgments The authors wish to thank the USGS, Animas abandoned mine lands (AML) team members who all provided useful discussions and data during preparation of this report. Special thanks to Stanley E. Church (USGS, ret.) who co-led the successful AML program. The Animas River Stakeholders Group, led by William Simon was inspirational in addressing watershed and mining-related issues in Silverton between 1996 and present. Roland J. Viger (USGS) provided useful guidance in using the GIS Weasel software. Denise Dundon provided GIS support. USGS reviewers Mary Ellen Benson, Eric Anderson and two anonymous external reviewers provided useful critique of this work. This study was supported by the U.S. Geological Survey Mineral Resources Program, the Mineral Environmental Assessment Methodologies Project and the Central Mineral and Environmental Resources Science Center. Any use of trade, product, or firm names is for descriptive purposes only and does not imply endorsement by the US Government.

Open Access This article is distributed under the terms of the Creative Commons Attribution License which permits any use, distribution, and reproduction in any medium, provided the original author(s) and the source are credited.

References

- Bejnar W (1957) Lithologic control of ore deposits in the southwestern San Juan Mountains. In: Kottlowski FE, Baldwin B (eds) Guidebook of southwestern San Juan Mountains, Colorado. New Mexico Geological Society 8th Annual Field Conference Guidebook, pp 162–173
- Besser JM, Finger SE, Church SE (2007) Impacts of historical mining on aquatic systems—An ecological risk assessment, chapter D. In: Church SE, von Guerard P, Finger SE (eds) Integrated investigations of environmental effects of historical mining in the Animas River watershed, San Juan County, Colorado. U.S. Geological Survey Professional Paper 1651, pp 87–106
- Bove DJ, Hon K, Budding KE, Slack JF, Snee LW, Yeoman RA (2001) Geochronology and geology of late Oligocene through Miocene volcanism and mineralization in the western San Juan Mountains, Colorado. U.S. Geological Survey Professional Paper 1642
- Bove DJ, Yager DB, Mast MA, Dalton JB (2007a) Alteration map showing major faults and veins and associated water-quality signatures of the Animas River watershed headwaters near Silverton, southwest Colorado. U.S. Geological Survey Scientific Investigations Map 2976, 18-p pamphlet, 1 plate, scale 1:24,000
- Bove DJ, Mast MA, Dalton JB, Wright WG, Yager DB (2007b) Major styles of mineralization and hydrothermal alteration and related solid and aqueous-phase geochemical signatures, chapter E3. In: Church SE, von Guerard P, Finger SE (eds) Integrated Investigations of Environmental Effects of Historical Mining in the Animas River Watershed, San Juan County, Colorado. U.S. Geological Survey Professional Paper 1651, pp 161–230
- Bruns DA (2005) Macroinvertebrate response to land cover, habitat, and water chemistry in a mining-impacted river ecosystem: 1 A GIS watershed analysis. *Aquat Sci* 67:403–423
- Burbank WS (1960) Pre-ore propylization, Silverton Caldera, Colorado. In: Geological Survey Research 1960. U.S. Geological Survey Professional Paper 400–B, article 6, pp B12–B13
- Casadevall TJ, Ohmoto H (1977) Sunnyside Mine, Eureka mining district, San Juan County, Colorado—Geochemistry of gold and base metal ore deposition in a volcanic environment. *Econ Geol* 92:1285–1320
- Chapman SS, Griffith GE, Omernik JM, Price AB, Freeouf J, Schrupp DL (2006) Ecoregions of Colorado (color poster with map, descriptive text, summary tables, and photographs). Reston, Virginia, U.S. Geological Survey (map scale 1:1,200,000)
- Church SE, von Guerard P, and Finger SE (eds) (2007) Integrated investigations of environmental effects of historical mining in the Animas River watershed, vol 1, 2. San Juan County, Colorado. U.S. Geological Survey Professional Paper 1651
- Clow DW, Sucker JK (2000) Relations between basin characteristics and stream water chemistry in alpine/subalpine basins in Rocky Mountain National Park, Colorado. *Water Resour Res* 36(1):49–61
- Dalton JB, Bove DJ, Mladinich CS, Rockwell BW (2007) Imaging spectroscopy applied to the Animas River watershed and Silverton caldera, chapter E2. In: Church SE, von Guerard P, Finger SE (eds) Integrated investigations of environmental effects of historical mining in the Animas River watershed, San Juan County, Colorado. U.S. Geological Survey Professional Paper 1651, pp 141–159
- DeGraff JV (2007) Addressing the toxic legacy of abandoned mines on public land in the western United States. *Rev Eng Geol* 17:1–8
- Earth Remote Sensing Data Analysis Center (ERSDAC) (2005) ASTER user's guide, part 1, General, Version 4.0: http://www.science.aster.ersdac.jspacesystems.or.jp/en/documnts/users_guide/part1/pdf/Part1_4E.pdf. Accessed 8 November 2012
- Helsel DR, Hirsch RM (2002) Statistical Methods in water resources: techniques of water resources investigations, book 4, chapter A3. U.S. Geological Survey
- Hunt GR, Salisbury JW (1970) Visible and near-infrared spectra of minerals and rocks, I. Silicate minerals. *Mod Geol* 1:283–300
- Hunt GR, Salisbury JW (1971) Visible and near-infrared spectra of minerals and rocks, II. Carbonates. *Mod Geol* 2:23–30
- Jenson SK, Domingue JO (1988) Software tools to extract topographic structure from digital elevation data for geographic information system analysis: photogram. *Eng Remote Sens* 54(11):1593–1600
- Johnson RH (2007) Ground water flow modeling with sensitivity analyses to guide field data collection in a mountain watershed. *Ground Water Monit Remediat* 27(1):75–83
- Johnson RH, Yager DB (2006) Completion reports, core logs, and hydrologic data from wells and piezometers in Prospect gulch, San Juan County, Colorado. U.S. Geological Survey Open-File Report, of 2006-1030
- Kendall MG (1975) Rank correlation methods, 4th edn. Charles Griffin, London, p 202
- Kimball BA, Walton-Day K, Runkel RL (2007) Quantification of metal loading by tracer injection and synoptic sampling, 1996–2000, Chapter E9: In: Church SE, von Guerard P, Finger SE (eds) Integrated investigations of environmental effects of historical mining in the Animas River watershed, San Juan County, Colorado. U.S. Geological Survey Professional Paper 1651, pp 417–495
- Kinnell PIA (2005) Raindrop-impact-induced erosion processes and prediction: a review. *Hydrol Process* 19:2815–2844
- Leib KJ, Mast MA, Wright WG (2007) Characterization of mainstem streams using water-quality profiles, chapter E11. In: Church SE, von Guerard P, Finger SE (eds) Integrated investigations of environmental effects of historical mining in the Animas River watershed, San Juan County, Colorado. U.S. Geological Survey Professional Paper 1651, pp 543–570
- Mast MA, Evans JB, Leib KJ, Wright WG (2000a) Hydrologic and water-quality data at selected sites in the upper Animas River watershed, southwestern Colorado, 1997–99. U.S. Geological Survey Open-File Report 2000-53
- Mast MA, Verplanck PL, Yager DB, Wright WG, Bove DJ (2000b) Natural sources of metals to surface waters in the Upper Animas River Watershed, Colorado. In: Proceedings of the 5th International Conference on acid-rock drainage (ICARD). Society for Mining, Metallurgy, and Exploration, pp 513–522
- Mast MA, Verplanck PL, Wright WG, Bove DJ (2007) Characterization of background water quality, chapter E7. In: Church SE, von Guerard P, Finger SE (eds) Integrated investigations of environmental effects of historical mining in the Animas River watershed, San Juan County, Colorado. U.S. Geological Survey Professional Paper 1651, pp 347–386
- O'Callaghan JF, Mark DM (1984) The extraction of drainage networks from digital elevation data. *Comput Vis Graph Image Process* 28:323–344
- Rockwell BW (2009) Comparison of ASTER- and AVIRIS-derived mineral and vegetation maps of the White Horse replacement alunite deposit and surrounding area, Marysvale volcanic field, Utah. U.S. Geological Survey Scientific Investigations Report 2009-5117. <http://pubs.usgs.gov/sir/2009/5117/>. Accessed 8 November 2012
- Rockwell BW (2010) Evaluation of detailed and automated methodologies for hydrothermal alteration mapping from space: application to geoenvironmental and mineral resource assessments at the scale of watersheds and permissive tracts. *Geol Soc Am Abstr Program* 42(5):214. Presentation handout at:

- http://gsa.confex.com/gsa/2010AM/finalprogram/abstract_1798_92.htm. Accessed 8 November 2012
- Schmidt TS, Church SE, Clements WH, Mitchell K, Fey DL, Wanty RB, Verplanck PL, San Juan CA, Klein TL, DeWitt EH, Rockwell BW (2009) Geologic processes influence the effect of mining on aquatic ecosystems. In: Webb RMT, Semmens DJ (eds) *Planning for an uncertain future—monitoring, integration, and adaptation*. Proceedings of the Third Interagency Conference on Research in the Watersheds. U.S. Geological Survey Scientific Investigations Report 2009-5049
- Schmidt TS, Wanty RB, Verplanck PL, Church SE, San Juan CA, Fey D, Rockwell BW, deWitt EH, Klein TL (2010) Predicting risks to aquatic life based on lithologic specific geochemical baselines. *Geol Soc Am Abstr Program* 42(5):214
- Sliva L, Williams D (2001) Buffer zone versus whole catchment approaches to studying land use impact on river water quality. *Water Res* 35(14):3462–3472
- Smith BD, McDougal RR, Deszcz-Pan M, Yager DB (2007) Helicopter electromagnetic and magnetic surveys, Chapter E4. In: Church SE, von Guerard P, Finger SE (eds) *Integrated investigations of environmental effects of historical mining in the Animas River watershed, San Juan County, Colorado*. U.S. Geological Survey Professional Paper 1651, pp 231–254
- Sole, TC, Grannito, Matthew, Rich, CL, Litke DW, Pellier RT (2007) Digital databases and CD-ROM for the Animas River watershed, Chapter G. In: Church SE, von Guerard P, Finger SE (eds) *Integrated investigations of environmental effects of historical mining in the Animas River watershed, San Juan County, Colorado*. U.S. Geological Survey Professional Paper 1651, pp 1079–1096
- Theil H (1950) A rank-invariant method of linear and polynomial regression analysis, vol 1, 2, and 3. *Ned. Akad. Wentsch Proc.*, 53:386–392, 521–525, and 1397–1412
- Varnes DJ (1963) *Geology and ore deposits of the south Silverton mining area, San Juan County, Colorado*. U.S. Geological Survey Professional Paper 378–A
- Viger RJ (2008) The GIS Weasel: an interface for the development of geographic information used in environmental simulation modeling. *Comput Geosci* 34(8):891–901
- Viger RJ, Leavesley GH (2007) The GIS Weasel user's manual. U.S. Geological Survey Techniques and Methods, book 6, chapter B4. <http://pubs.usgs.gov/tm/2007/06B04/>. Accessed 8 November 2012
- Viger RJ, Markstrom SL, Leavesley GH (1998) The GIS Weasel—an interface for the treatment of spatial information used in watershed modeling and water resources management. In: *Proceedings of the First Federal Interagency Hydrologic Modeling Conference, April 19–23, 1998, Las Vegas, Nev.*, 2(7):73–80
- Wang X, Yin ZY (1997) Using GIS to assess the relationship between land use on water quality at a watershed level. *Environ Int* 23:103–114
- Wright WG, Simon W, Bove DJ, Mast MA, Leib KJ (2007) Distribution of pH values and dissolved trace-metal concentrations in streams, Chapter E10. In: Church SE, von Guerard P, Finger SE (eds) *Integrated investigations of environmental effects of historical mining in the Animas River watershed, San Juan County, Colorado*. U.S. Geological Survey Professional Paper 1651, pp 497–541
- Yager DB (2008) Environmental rock properties at abandoned mine lands that generate or neutralize acid drainage, Silverton, Colorado, chapter K. In: Verplanck PL (ed) *Understanding contaminants associated with mineral deposits*. U.S. Geological Survey Circular 1328, pp 64–69
- Yager DB, Bove DJ (2002) Generalized geologic map of the Upper Animas River Watershed and Vicinity, Silverton, Colorado. U.S. Geological Survey Miscellaneous Field Studies Map MF-2377, U.S. Geological Survey, Denver, CO, scale 1:48,000
- Yager DB, Bove DJ (2007) Geologic framework, chapter E1. In: Church SE, von Guerard P, Finger SE (eds) *Integrated investigations of environmental effects of historical mining in the Animas River watershed, San Juan County, Colorado*. U.S. Geological Survey Professional Paper 1651, pp 107–140
- Yager DB, Caine JS (2003) GIS analysis of the fundamental geologic, topographic, and mining-related factors that influence water quality in the upper Animas River watershed, Silverton, Colorado. *Geological Society of America, Rocky Mountain Section, 55th Annual Meeting Abstr. Program*. 35(5):6
- Yager DB, Mast MA, Verplanck PL, Bove DJ, Wright WG, Hageman PL (2000) Natural versus mining-related water quality degradation to tributaries draining Mount Moly, Silverton, CO. In: *Proceedings of the Fifth International Conference on Acid Rock Drainage, Society for Mining, Metallurgy, and Exploration, Inc., Littleton*, pp 535–547
- Yager DB, Caine JS, Bove DJ, Church SE, Smith BD, McDougal RR, Wirt L, Mast MA, Kimball BA, Walton-Day K (2002) A GIS data viewer for physical and geochemical characterization of abandoned mine lands: an example from the Animas River watershed, Silverton, Colorado. *Geol Soc Am Annu Meet Abstr Program* 34(6):145
- Yager DB, McCafferty AE, Stanton MR, Diehl SF, Driscoll RL, Fey DL, Sutley SJ (2005) Net acid production, acid neutralizing capacity, and associated geophysical, mineralogical, and geochemical characteristics of Animas River watershed rocks near Silverton, Colorado. U.S. Geological Survey Open-File Report 2005-1433
- Yager DB, Choate L, Stanton MR (2008) Net acid production, acid neutralizing capacity, and associated mineralogical and geochemical characteristics of Animas River watershed igneous rocks near Silverton, Colorado. U.S. Geological Survey Scientific Investigations Report 2008-5063
- Yager DB, Johnson RH, Smith BD (2008) Using a geographic information system (GIS) to determine the physical factors that affect water quality in the western San Juan Mountains, Silverton, Colorado, chapter M. In: Verplanck PL (ed) *Understanding contaminants associated with mineral deposits*. U.S. Geological Survey Circular 1328, pp 76–83
- Yager DB, Stanton MR, Choate LM, Burchell A (2009) Acid neutralizing capacity and leachate results for igneous rocks, with associated carbon contents of derived soils, Animas AML site, Silverton, Colorado. In: Barnheisel RI (ed) *Revitalizing the Environment: Proven Solutions and Innovative Approaches: National Meeting of the American Society of Mining and Reclamation, Billings, MT, May 30–June, 5, 2009*, ASMR publication, Lexington, pp 1662–1697
- Yager DB, Burchell A, Johnson RH (2010) A geologic and anthropogenic journey from the Precambrian to the new energy economy through the San Juan volcanic field. In: Morgan LA, Quane SL (eds) *Through the Generations: Geologic and Anthropogenic Field Excursions in the Rocky Mountains from Modern to Ancient: Geol Soc Am, Field Guide* 18, pp 193–237